catalysts

MDPI

Review

Advances in Chitosanase Research: From Structure and Function to Green Biocatalytic Production of Chitooligosaccharides

Oanh Thi Kim Nguyen [1,2,3], Parushi Nargotra [1], Po-Ting Chen [4], Chwen-Jen Shieh [5], Yung-Chuan Liu [6,*] and Chia-Hung Kuo [1,2,7,*]

[1] Department of Seafood Science, National Kaohsiung University of Science and Technology, Kaohsiung 811, Taiwan; i112180115@nkust.edu.tw (O.T.K.N.); parushi11nargotra@gmail.com (P.N.)
[2] Institute of Aquatic Science and Technology, National Kaohsiung University of Science and Technology, Kaohsiung 811, Taiwan
[3] Faculty of Food Science and Technology, Ho Chi Minh City University of Industry and Trade, Ho Chi Minh City 700000, Vietnam
[4] Department of Biotechnology and Food Technology, Southern Taiwan University of Science and Technology, Tainan 71005, Taiwan; ptchen@stust.edu.tw
[5] Biotechnology Center, National Chung Hsing University, Taichung 402, Taiwan; cjshieh@nchu.edu.tw
[6] Department of Chemical Engineering, National Chung Hsing University, Taichung 402, Taiwan
[7] Center for Aquatic Products Inspection Service, National Kaohsiung University of Science and Technology, Kaohsiung 811, Taiwan
* Correspondence: ycliu@dragon.nchu.edu.tw (Y.-C.L.); kuoch@nkust.edu.tw (C.-H.K.); Tel.: +886-4-22853769 (Y.-C.L.); +886-7-3617141 (ext. 23646) (C.-H.K.); Fax: +886-4-22854734 (Y.-C.L.); +886-7-3640634 (C.-H.K.)

Abstract

Chitosanases are glycoside hydrolases (GHs) that catalyze the endo- or exo-type cleavage of β-1,4-glycosidic linkages in chitosan, enabling the selective production of chitooligosaccharides (COSs) with well-defined structures and diverse bioactivities. Owing to their substrate specificity and environmentally friendly catalytic action, chitosanases have garnered increasing attention as sustainable biocatalysts for COS production, with broad application potential in agriculture, food, medicine, and cosmetics. This review provides a comprehensive overview of recent advances in chitosanase research, focusing on the catalytic mechanisms and structure–function relationships that govern substrate selectivity and functional divergence across different GH families. Microbial diversity and heterologous expression systems for chitosanase production are discussed in parallel with biochemical characterization to support the rational selection of enzymes for specific biotechnological applications. Advances in protein engineering and computational approaches are highlighted as strategies to improve catalytic efficiency, substrate range, and stability. In addition, bioprocess optimization is addressed, with emphasis on fermentation using low-cost substrates and the application of immobilized enzymes and nano-biocatalyst systems for green and efficient COS production. Summarizing and discussing previous findings are essential to support future research and facilitate the development of next-generation chitosanases for sustainable industrial use.

Keywords: chitosanase; chitooligosaccharides; structure–function relationship; protein engineering; fermentation; green biocatalysis

check for updates

Academic Editor: Evangelos Topakas

Received: 13 August 2025
Revised: 2 September 2025
Accepted: 4 September 2025
Published: 6 September 2025

Citation: Nguyen, O.T.K.; Nargotra, P.; Chen, P.-T.; Shieh, C.-J.; Liu, Y.-C.; Kuo, C.-H. Advances in Chitosanase Research: From Structure and Function to Green Biocatalytic Production of Chitooligosaccharides. *Catalysts* **2025**, *15*, 863. https://doi.org/10.3390/catal15090863

Copyright: © 2025 by the authors. Licensee MDPI, Basel, Switzerland. This article is an open access article distributed under the terms and conditions of the Creative Commons Attribution (CC BY) license (https://creativecommons.org/licenses/by/4.0/).

1. Introduction

Chitosan, a linear polysaccharide derived from the partial deacetylation of chitin, has gained substantial attention due to its biocompatibility, biodegradability, and diverse biological activities. However, the limited solubility of chitosan under neutral conditions has prompted growing interest in its low-molecular-weight derivatives, namely chitooligosaccharides (COSs) [1]. These COSs exhibit enhanced physicochemical properties and bioactivities, including antioxidant, antimicrobial, anti-inflammatory, and antitumor effects, making them promising candidates for applications in food, agriculture, biomedicine, and cosmetics [2]. The enzymatic degradation of chitosan using chitosanases represents an eco-friendly and highly specific route for the controlled production of COSs with defined degrees of polymerization (DP), acetylation patterns, and sequence arrangements. The main forms of chitosanase enzymes can be categorized based on their mode of action and product. Endo-chitosanases (EC 3.2.1.132), a group of GHs, catalyze the endo-type cleavage of β-1,4-glycosidic bonds of D-glucosamine (GlcN) and/or N-acetyl-D-glucosamine (GlcNAc) in chitosan chains [3]. Exo-chitobiohydrolase or exo-chitosanases release $(GlcN)_2$ from the chain ends of chitosan. Exo-*β*-D-glucosaminidase predominantly acts on the non-reducing end of polymeric chitosan or oligomeric COSs, resulting in the production of GlcN [4]. These enzymes are taxonomically and mechanistically diverse, classified into several GH families, including GH5, GH7, GH8, GH46, GH75, and GH80, each exhibiting distinct structural folds, catalytic mechanisms, and substrate preferences [5].

In recent years, considerable efforts have focused on elucidating the catalytic mechanisms of chitosanases with particular emphasis on the structural determinants that govern substrate selectivity, cleavage patterns, and product profiles. Advances in structural biology supported by protein engineering [6–10] and computational modeling [11–14] have provided valuable insights into the organization of catalytic clefts and subsite architectures, which underpin functional divergence across GH families. Building on these insights, protein engineering efforts aimed at enhancing catalytic performance and stability are increasingly guided by in silico design approaches, which leverage molecular docking, molecular dynamics simulations, and structural modeling to enable the rational redesign of chitosanases.

At the same time, the exploration of microbial sources including bacteria, fungi, and actinomycetes has expanded the diversity of chitosanases [15], while heterologous expression systems have enabled scalable enzyme production. These developments, together with advances in the understanding of chitosanase biochemical properties such as substrate specificity, kinetics, and physicochemical stability, provide a foundation for optimizing COS production tailored to specific functional applications.

From an industrial perspective, sustainable bioprocessing strategies have been increasingly prioritized. The use of low-cost substrates, such as seafood processing byproducts, not only reduces production costs but also contributes to circular bioeconomy goals. Additionally, immobilized chitosanase systems and nano-biocatalysts offer improved enzyme stability, reusability, and process efficiency, aligning with green chemistry principles.

This review aims to provide a comprehensive and up-to-date overview of chitosanases, with a focus on their catalytic mechanisms, structure–function relationships, microbial production systems, kinetic behavior, protein engineering strategies, and bioprocess optimization. Emphasis is placed on the integration of recent advances in enzymology, structural biology, and green biocatalysis to support the rational development of chitosanase-based platforms for the sustainable and value-added production of functional COSs.

2. Chitosanases

Chitosanases are glycoside hydrolases (GHs) that cleave the β-1,4-glycosidic linkages in chitosan, a partially deacetylated derivative of chitin. Based on their cleavage positions, they can be divided into endo- and exo-chitosanases. While the former are more prevalent and have been studied more extensively due to their capacity to generate COSs with defined DP (Figure 1A), the latter are described to act on chitosan chains from the non-reducing end to release $(GlcN)_2$ by exo-chitosanase or GlcN by Exo-*β*-D-glucosaminidase (Figure 1B). Exo-*β*-D-glucosaminidases are exo-type chitosanases that release GlcN monomers from the non-reducing ends, and have been identified in only a few microorganisms, such as *Aspergillus fumigatus*, *Aspergillus spp.*, *Trichoderma reesei*, *Penicillium funiculosum*, *Nocardia orientalis*, and *Thermococcus kodakaraensis* [16]. The catalytic mechanisms and substrate recognition modes of chitosanases are highly diverse across GH families, reflecting their structural and functional specialization. This section provides an overview of the enzyme mechanisms and structure–function determinants of substrate selectivity.

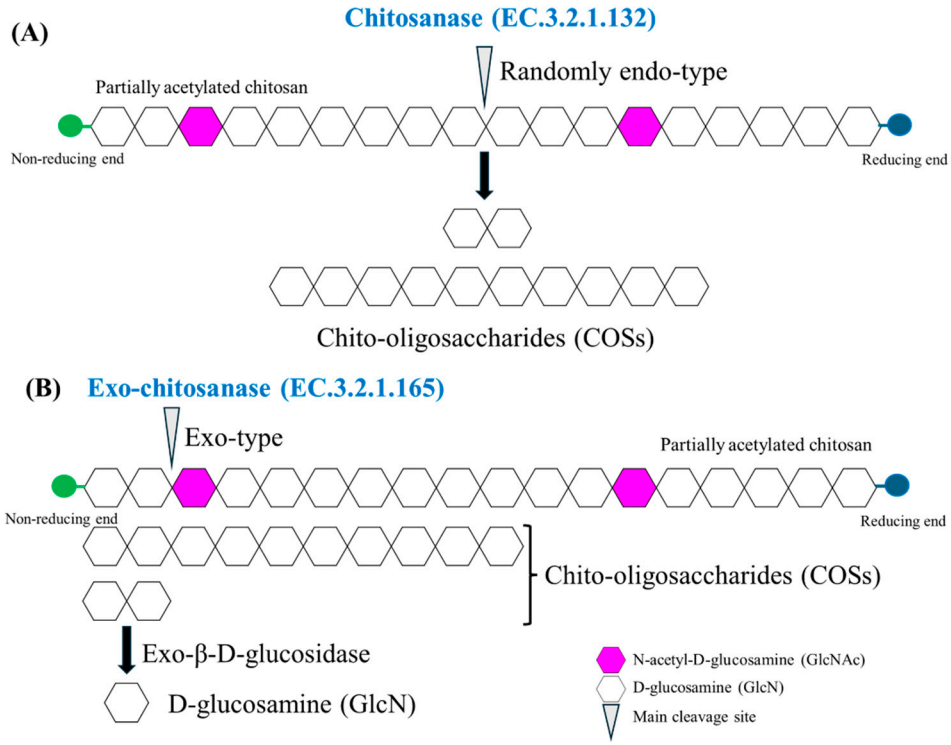

Figure 1. Mode of action of (**A**) endo- and (**B**) exo- chitosanase.

2.1. Catalytic Mechanisms of Chitosanases

Chitosanases exhibit distinct catalytic mechanisms across GH families, which are generally categorized as either inverting or retaining enzymes. These mechanistic differences arise from variations in active site architecture and catalytic residue positioning. According to the CAZyme database, inverting chitosanases from the GH8 and GH46 families catalyze glycosidic bond cleavage through a single-step acid/base mechanism. In contrast, retaining chitosanases from members of GH2 and GH5 operate via a two-step mechanism that involves the formation of a covalent glycosyl–enzyme intermediate. A detailed understanding of the associated catalytic features, such as proton transfer routes, catalytic dyads, and conformational dynamics, is essential for elucidating substrate specificity and for guiding structure-based enzyme engineering efforts.

The retaining mechanism is one of the two principal catalytic strategies employed by GHs and is characterized by the retention of the anomeric configuration in the hydrolysis

product. This mechanism follows a two-step reaction involving the formation of a covalent glycosyl–enzyme intermediate [17]. In the first step, two conserved carboxylate residues, typically a glutamate acting as a general acid and an aspartate as a nucleophile, coordinate at the −1 subsite. The glutamate protonates the glycosidic oxygen of the β-1,4-linkage, promoting cleavage of the glycosidic bond, while the aspartate attacks the anomeric carbon (C1) to form a transient covalent intermediate. Following intermediate formation, the leaving sugar moiety dissociates, and a water molecule enters the active site. In the second step, this water molecule is deprotonated by the glutamate (now functioning as a general base). The resulting hydroxide ion then attacks the C1 center, releases the final product and regenerates the enzyme to its original state. Since the nucleophilic attack by water occurs on the same side as the original leaving group, the stereochemistry at the anomeric center is retained throughout the reaction [18].

Conversely, the inverting mechanism operates via a single-step direct displacement reaction that results in inversion of the anomeric configuration [17]. This process also involves two catalytic residues, typically a general acid and a general base, strategically positioned approximately 10 Å apart to enable in-line nucleophilic attack. The mechanism begins with a water molecule positioned at the −1 subsite of the active site. A carboxylate residue, commonly aspartate, acts as a general base to deprotonate the water molecule, generates a nucleophilic hydroxide ion. Simultaneously, a second residue, typically glutamate, donates a proton to the glycosidic oxygen of the leaving group, thereby facilitating bond cleavage. The hydroxide ion attacks the anomeric carbon (C1) from the opposite face of the departing group. This results in inversion of stereochemistry at the anomeric center [18]. Additionally, chitosanases recognize chitosan chains with varying degrees of acetylation and this recognition influences their catalytic efficiency. Specifically, chitosanases interact with both GlcN and GlcNAc residues within the substrate-binding cleft, and their activity is modulated by the degree of acetylation (DA). Generally, a lower DA (GlcN-rich chains) favors stronger binding and higher catalytic rates, whereas higher DA (GlcNAc-rich chains) can reduce enzymatic activity due to steric and electronic effects [19,20].

2.2. Structure–Function Relationships: Substrate Selectivity and Functional Divergence

Understanding the relationship between structure and function of chitosanases is essential for the controllable preparation of COSs with specific DP. Substrate selectivity and functional divergence among chitosanases are governed by intricate structure–function relationships determined by their active-site architectures and subsite organization. Three-dimensional structures of representative chitosanases from different GH families are illustrated in Figure 2.

Recent structural elucidation of the GH8 chitosanase CSN-MN from *Bacillus* spec. MN provided detailed insights into the molecular determinants of substrate recognition. This enzyme adopts a typical $(\alpha/\alpha)_6$ barrel fold with a well-defined catalytic cleft extending across from subsites −3 to +3 and a putative (+4) subsite. The distance measured between the catalytic residues E74 and E261 during simulation was 7.4 Å, defining an inverting mechanism. The active site of CSN-MN exhibits a wide and open cleft typical of endo-acting enzymes, with a highly acidic electrostatic surface that favors binding of highly deacetylated substrates. Structural analyses identified residues D131 (−3), N260 (−2), D135 (−1), S198 (−1), and N271 (−1) as forming the most stable hydrogen bonds with the protonated GlcN units, indicating that subsites (−3) to (−1) play a dominant role in substrate binding and display a marked preference for GlcN. Notably, D135 and S198 at subsite (−1) are directly involved in hydrogen bonding with GlcN. Additionally, R274 stabilizes the positive charge and, together with D135 and S198, contributes to the formation of a compact surface on the inner side of the binding cavity. This spatial arrangement

constrains the accommodation of GlcNAc, which is strongly disfavored at subsites (−1), (−2), and (+1), tolerated slightly at (−3), and accepted to a limited extent at (+2) and (+3). These findings highlight the substrate selectivity of CSN-MN and support its functional specialization toward GlcN-rich oligomers [21].

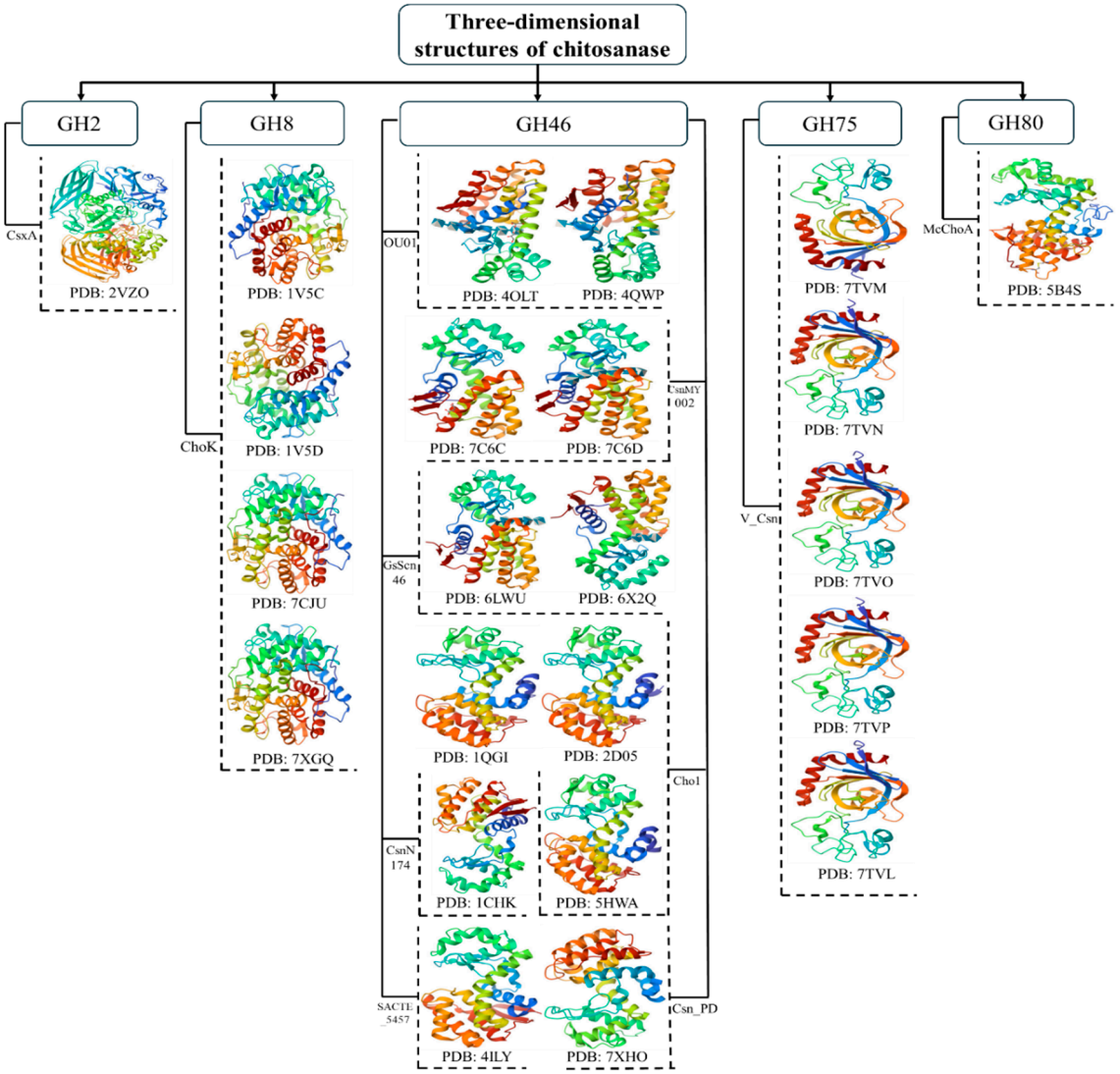

Figure 2. Three-dimensional structures of chitosanase with the corresponding PDB codes from https://www.rcsb.org/structure (accessed on 3 September 2025).

Regarding GH46, further structural insights are provided by the chitosanase GsCsn46A from *Gynuella sunshinyii* [22]. Its crystal structure reveals two domains comprising nine α-helices and two β-strands that form a closed cleft accommodating COSs between them. Structural analyses of GsCsn46A bound to chitotetraose and chitopentaose uncovered distinct interaction patterns at the negatively numbered subsites of the cleft. Comparison with the GH46 chitosanase OU01 showed that chitotetraose occupied subsites −4 to −1, while chitopentaose extended to an additional −5 subsite. These observations uncover the presence of previously unrecognized sugar-binding regions, specifically the −5 sugar residue and the novel −4 subsite, which lie beyond the canonical −3 to −1 subsites typically reported in GH46 enzymes. The findings confirm that the catalytic cleft of GsCsn46A can bind at least eight sugar residues, spanning from −5 to +3 subsites. This extended binding region suggests that GH46 enzymes may accommodate COSs with DP greater than six. In contrast, the GH46 endo-chitosanase OUC-CsnPa from *Paenibacillus* sp. 1–18 exhibits

distinct substrate selectivity and subsite-dependent digestion specificity, highlighting an unusual structure–function relationship within the GH46 family. Digestion pattern analysis showed that OUC-CsnPa is capable of producing monosaccharides from chitotetraose $(GlcN)_4$, the smallest substrate it recognizes, via a random endo-acting cleavage mechanism. This hydrolytic behavior is complemented by a transglycosylation capacity that contributes to the regulation of product abundance during chitosan degradation. Molecular docking studies revealed that OUC-CsnPa accommodates $(GlcN)_6$ across subsites −3 to +3. This interaction involves the conserved catalytic residues E104 and D122, along with several residues responsible for hydrogen bonding such as T116, R124, T127, T134, and Y215. The binding of $(GlcN)_4$, however, involved a distinct set of interactions, with structural rearrangements occurring at the negative subsites. Notably, two unique residues (D140 and G142) located in the insertion region N139–P143 at the roof of the catalytic cleft were found to play a crucial role in recognizing and stabilizing the GlcN unit at the −3 subsite through hydrogen bonding interactions of 3.4 Å and 3.2 Å, respectively. This interaction facilitates the rearrangement of $(GlcN)_4$ and its subsequent positioning from −1 to +3 subsites, enabling monosaccharide production from the tetrasaccharide substrate. Structural comparison with GsCsn46A from *Gynuella sunshinyii* demonstrated that the lack of such an insertion region in GsCsn46A resulted in $(GlcN)_4$ preferentially occupying subsites −2 to +2, consistent with a symmetric digestion mode and absence of monosaccharide generation. The insertion-derived protrusion in OUC-CsnPa represents a unique structural determinant that directly contributes to its distinct substrate-binding mode and catalytic specificity. This study elucidates subsite-level determinants responsible for monosaccharide production by an endo-chitosanase. The findings offer valuable insights into how structural variations in the active-site architecture of GH46 enzymes govern their functional divergence [23].

In GH5 research, the specificity of chitosanase–substrate interactions are also influenced by the chemical nature of the C-2 substituents on the sugar backbone. In the OUC-Csngly enzyme (GH5), structural analysis demonstrated different cleavage patterns toward COSs and cellooligosaccharides. This was observed in complexes with $(GlcN)_4$, where the amino group at C-2 was oriented outward from the catalytic cleft, facilitating interactions with Trp99 at the −3 subsite. In contrast, the hydroxyl group of cellotetraose was directed inward, forming a hydrogen bond with Trp323 at the −2 subsite. These configurations suggest that $(GlcN)_4$ spans subsites −3 to +1, while tighter engagement of cellotetraose facilitates complete hydrolysis. Functionally, OUC-Csngly exhibited atypical endo-type activity that generated mono- and disaccharides from chitosan or COSs, an activity more commonly associated with exo-glucosaminidases. The enzyme cleaved $(GlcN)_4$ through two distinct modes, attributed to its capacity to engage both −2 and −3 subsites depending on substrate orientation. Moreover, it catalyzed not only hydrolysis but also transglycosylation of cellooligosaccharides, highlighting its catalytic versatility. These variations in product profiles underscore the critical role of C-2 substituents in determining substrate orientation, subsite occupancy and catalytic trajectory [24].

For GH75, structural modeling and molecular dynamics simulations of the chitosanase from *Aspergillus fumigatus* revealed critical insights into the effects of temperature on its structure and function. The predicted structure, validated through multiple evaluation tools, exhibits a narrow catalytic cleft shaped by loops 3, 6, and 11, where the catalytic residues Asp143 and Glu152 are positioned almost at the center of the binding site. Docking analysis confirmed that the cleft geometry is well-matched to the dimensions of DP6-chitosan, based on the length and narrowest width of the binding site. Structural alignment with the viral GH75 enzyme V-Csn revealed a high degree of conservation in overall fold and active-site configuration despite low sequence similarity. This observation points to a possible case of evolutionary convergence. Importantly, the key substrate-binding residues

are located in highly flexible loops (3, 6, 11), and their conformational changes at high temperature, especially the transition from open to closed states, can hinder substrate binding. These observations provide a mechanistic explanation for the loss of activity stability of *A. fumigatus* chitosanase. The analysis provides directions for modifying thermal stability and enables the investigation of a large number of proteins lacking experimental structures [13].

3. Chitosanase-Producing Microorganisms and Expression Systems

3.1. Microbial Sources of Chitosanases

Chitosanases are responsible for the specific hydrolysis of chitosan. These enzymes have been identified across various biological sources, including microorganisms such as bacteria, fungi, and actinomycetes, as well as in viruses and certain higher plants. Among these sources, microorganisms represent the most versatile producers, having evolved chitosanase-based systems for efficient chitosan degradation [25].

3.1.1. Bacterial Chitosanases

Bacteria represent one of the most prolific and diverse sources of chitosanases, with numerous genera reported to possess chitosan-degrading capacity, including *Bacillus* sp., *Serratia* sp., *Pseudomonas* sp., *Staphylococcus* sp., and *Paenibacillus* sp. These bacteria were studied most extensively as a chitosanase source even up to structural and molecular level, making it suitable for molecular cloning and heterologous expression. Bacterial chitosanases are typically classified into GH families 8, 46, and 80, and often exhibit efficient hydrolytic activity under neutral to slightly alkaline conditions. Several bacterial strains have been successfully isolated from soil or marine environments and even from seafood waste. For instance, *Serratia marcescens* TKU011, *Paenibacillus* sp. TKU047, and *Acinetobacter calcoaceticus* TKU024 were obtained from soil habitats and possess the ability to utilize seafood processing wastes as the sole carbon/nitrogen sources, instead of relying on purified chitosan. In particular, TKU011 produced the highest chitosanase activity when cultivated on shrimp shell waste, and its culture supernatant also exhibited antioxidant activity [26]. Wang et al. [27] reported the purification of two chitosanases (CHSA1 and CHSA2) from the culture supernatant of *Acinetobacter calcoaceticus* TKU024 grown in medium containing squid pens as the sole carbon/nitrogen source. Similarly, chitosanase production by *Paenibacillus* sp. TKU047 was achieved using 2% squid pen powder as the sole carbon/nitrogen source [28,29]. These results demonstrate that the TKU strains differ from conventional chitosan-dependent microorganisms and offer promising potential for low-cost production of bioactive COSs. The chitosanase *Bp*CSN, produced by *Bacillus paramycoides* BP-N07 isolated from marine mud, exhibits high activity and stability, making it a promising candidate for industrial-scale COS production [30]. *Serratia* sp. QD07 obtained from deep-sea mud produced CsnS as a new member of GH-46 chitosanase, using chitosan as an inducer for chitosanase production. CsnS exhibits favorable properties and may have potential applications in the production of bioactive COSs in the food and pharmaceutical industries [31]. Furthermore, chitosanase-producing microorganisms have also been isolated from seafood waste environments. *B. cereus* TY24 obtained from shrimp and crab shell compost produces chitosanase (CHOE) with potential for chitosan bioutilization [32]. *Bacillus subtilis* CH2, isolated from the intestine of scorpion fish, exhibited the highest chitosanase activity when fructose was used as the carbon source, differing from most strains that require chitosan for induction. The highly active enzyme from *B. subtilis* CH2 could be useful in the industries under suitable enzyme conditions [33].

These bacteria can secrete chitosanase into the culture medium under relatively simple fermentation conditions, facilitating downstream purification and characterization. Further-

more, in addition to conventional laboratory media, alternative low-cost substrates such as squid pens and shrimp shells have been employed as inducers for chitosanase production in bacteria [34,35]. This not only reflects the metabolic flexibility of bacterial strains but also aligns with sustainable bioprocessing approaches by utilizing agro-industrial waste.

3.1.2. Fungal Chitosanases

Filamentous fungi represent an important microbial source of chitosanase with the predominant of GH75 chitosanases, with reported genera including *Aspergillus*, *Penicillium*, *Fusarium*, *Gongronella*, *Mucor*, and *Chaetomium* [36]. Numerous investigations have demonstrated that fungal strains capable of chitosan hydrolysis are promising sources for chitosanase production. Notably, *Aspergillus fumigatus* strain 2T-2 isolated from soil demonstrated considerable chitosanase activity when cultivated in media containing powdered chitosan as the sole carbon source. Enzymatic hydrolysis by this strain yielded both COSs and glucosamine salts, indicating its potential for the tailored production of diverse chitosan-derived bioactives [15]. Another study conducted by Cao et al. demonstrated that *Penicillium oxalicum* M2, recovered from bird fecal samples, produced a chitosanase with high catalytic activity. This result provides evidence for its applicability in industrial-scale COS production [37]. *Penicillium janthinellum* D4, isolated from the soil, produced D4 chitosanase when cultured in medium supplemented with squid pen powder. Production of chitooligomers with DP 3–9 by the enzyme indicates its suitability for synthesizing functional COSs. [38]. In another study, *Fusarium oxysporum* D18, also isolated from soil, exhibited effective chitosanase production under solid-state fermentation using shrimp processing waste as substrate. The resulting COSs demonstrated antitumor activity and showed potential for therapeutic applications [39]. Additionally, *Chaetomium globosum* KM651986, isolated from shrimp shell waste, exhibited high chitosanase activity under solid-state fermentation using wheat bran supplemented with 1% soluble chitosan. The COSs generated by this strain exhibited antioxidant and antimicrobial activities, making the enzyme a promising biocatalyst for pharmaceutical applications [40].

3.1.3. Actinomycetes Chitosanases

Actinomycetes, a phylogenetically diverse group of Gram-positive filamentous bacteria represent an important microbial source of chitosanases, with *Streptomyces* species being particularly prominent. These soil-dwelling organisms are attractive for industrial applications due to their metabolic versatility and secretion capacity. A soil-derived *Streptomyces* strain was reported to produce a bifunctional chitosanase capable of degrading both chitosan and cellulose-based substrates. The enzyme exhibited antioxidant activity in the resulting oligosaccharides, which highlights its potential for the large-scale production of biofunctional COSs relevant to agriculture, waste management, and bioprocessing industries [41]. In a separate study, *Streptomyces roseolus* DH, isolated from shrimp-shell-enriched soils, was cultivated in a chitin-containing medium supplemented with chitinase to induce chitosanase production. This enzyme primarily yielded chitotrisaccharides. The resulting product uniformity reflects its suitability for applications that demand consistent COS structures [42]. Additionally, *Streptomyces* sp SA4, recovered from biowaste soil, demonstrated high chitosanase productivity when cultured with xylose and sucrose as carbon sources, which is an important consideration for cost-effective industrial fermentation. The resulting COSs exhibited strong antibacterial activity and showed promise in biomedical applications, particularly in the treatment of diabetic foot ulcers [43].

3.2. Heterologous Expression Systems

Although native microbial strains are valuable for chitosanase production, their practical application in industrial enzyme production remains constrained due to slow growth

rates, limited enzyme activity, and poor expression yields. Heterologous expression systems offer a promising alternative, enabling high-yield production and facilitating molecular modifications to enhance enzyme activity and stability [44]. Therefore, the development of effective expression systems is critical for large-scale production, protein engineering, and bioprocess optimization. Various hosts such as *Escherichia coli* (*E. coli*), *Pichia pastoris*, and *Bacillus subtilis* have been successfully employed for recombinant chitosanases expression, each offering distinct advantages and limitations (Table 1).

Table 1. Advantages and limitations of common heterologous expression systems for recombinant chitosanases.

Expression Host System	Advantages	Limitations	References
E. coli	Rapid growth; high-cell-density cultivation; low-cost media; ease of genetic manipulation	Protein overexpression may impose metabolic burden; limited folding of complex proteins	[45]
Bacillus subtilis	Non-pathogenic; genetically well-characterized; strong protein secretion; suitable for industrial fermentation	Expression efficiency is strain-dependent; extracellular proteases may degrade recombinant proteins	[46]
P. pastoris	Eukaryotic folding and glycosylation; high-cell-density fermentation; efficient secretion of active enzymes	Requires methanol induction; relatively long cultivation times; higher cost and operational complexity	[47]

Among prokaryotic hosts, *E. coli* is the most extensively utilized expression system for chitosanases due to its rapid growth, genetic tractability, high protein yield, short fermentation time, and low-cost cultivation requirements [32]. For instance, a GH46 chitosanase OUC-CsnPT, derived from *Paenibacillus tyrfis*, exhibited an exceptionally high specific activity of 5346.56 U/mg, surpassing most reported chitosanases (Table 1). It catalyzed the production of GlcN and $(GlcN)_2$ via an endo-type cleavage mechanism. This mode of action facilitates applications with higher added value [48]. GsCsn46A, another GH46 chitosanase from *Gynuella sunshinyii* displayed a specific activity of 260.87 U/mg with distinct cold-adapted characteristic. This provided a more environmentally friendly approach for the controlled production of COSs with DP 2–7, 2–5, and 2–3, achieving corresponding yields of 70.9%, 87.1%, and 94.6% after 0.5, 2, and 6 h. Its excellent properties may render the enzyme highly applicable in various aspects of COS industrial manufacturing [49]. While most GH46 chitosanases exhibit endo-type cleavage activity, a novel recombinant enzyme (Csn21c) derived from *Streptomyces alblongus* was found to display an exo-type cleavage pattern, which is rarely observed among GH46 enzymes. Csn21c exhibited a specific activity of 336.2 U/mg with optimal catalytic performance at alkaline pH 8.0, in contrast to the majority of previously characterized chitosanases, which function most efficiently under acidic to neutral conditions (pH 4–7). This property highlights its potential for efficient glucosamine and COS production under industrially relevant conditions [50]. In addition, CscB, a novel GH46 endo-type chitosanase cloned from *Kitasatospora setae* KM-6054, exhibited maximal activity (1094.21 U/mg) along with cold-adapted characteristics, strong substrate affinity, and high catalytic efficiency. These properties reinforce its promise as a biocatalyst for sustainable production of low-DP COSs (DP 2–4) with commercial potential [51].

Bacillus subtilis has gained attention as an efficient prokaryotic host for heterologous expression of chitosanases, owing to its generally recognized as safe (GRAS) status, high secretory capacity, lack of endotoxins, and minimal codon usage bias [52]. Both chitosanases Csn from *Bacillus subtilis* 168 and PbCsn8 from *Paenibacillus barengoltzii* were heterologously expressed in *B. subtilis* as extracellular proteins. Csn, a GH46 enzyme, achieved a maximum specific activity of 208.23 U/mL in a 5 L fermenter after 24 h and efficiently hydrolyzed both α- and β-chitosan into low-molecular-weight COSs, mainly dimers to tetramers. These findings demonstrate the efficiency of *B. subtilis* as a secretion host and highlight its potential for industrial-scale COS production [53]. Meanwhile, PbCsn8 reached a maximal yield of 1,108 U/mL with protein content of 4.7 mg/mL after incubation for 84 h under high-cell-density fermentation in a 5-L bioreactor. This enzyme demonstrated a specific activity of 360.4 U/mg and efficiently converted chitosan to COSs with the high yield of 79.3%, demonstrating its promise for industrial applications [25].

On the other hand, *Pichia pastoris* offers a eukaryotic expression system for chitosanase production owing to its ability to achieve high-level heterologous protein expression while secreting minimal endogenous proteins [54], which may significantly reduce downstream processing costs [55]. BaCsn46B, a heterologously expressed GH46 chitosanase, exhibits high extracellular production, reaching 8907.2 U/mL activity and 4.5 g/L of secreted protein. The purified enzyme shows a specific activity of 2380.5 U/mg under optimal conditions (pH 6.5, 55 °C). Its notable thermostability and pH tolerance support efficient chitosan hydrolysis into diverse COSs. These properties make BaCsn46B as a strong candidate for industrial-scale COS production [56]. Likewise, a GH5 chitosanase (Csn5) from *Streptomyces griseus* HUT 6037 also attained an enzymatic activity of 90.62 U/mL following 96 h of high-density fermentation. When applied to COS production, the crude enzyme (20 U/mL) achieved a hydrolysis rate of 91.2% within 8 h, yielding COSs predominantly of DP 2–4 [57]. It enabled efficient expression of both wild-type and mutant forms of the chitosanase SsCsn46 from *Streptomyces* sp. N174. Following 96 h of methanol induction in a 5 L fermenter, the wild-type enzyme was expressed at 5.7 mg/mL with a specific activity of 50,000 U/mg, while the mutant variant (m-SsCsn46) reached a higher expression level of 8.5 mg/mL but with a reduced specific activity of 30,000 U/mg. Despite the decline in catalytic efficiency, m-SsCsn46 exhibited a narrower product profile, primarily yielding chitopentasaccharides (DP5), which have been associated with improved gut microbiota. In contrast, the wild-type enzyme produced a broader range of oligomers (DP3–5). This enhanced product uniformity significantly reduces downstream purification demands and operational costs. The use of high-value mutant chitosanases expressed in *P. pastoris* represents a promising strategy for the efficient production of high-purity oligosaccharides for pharmaceutical applications [58].

Overall, the choice of expression system should be aligned with the enzyme's structural features, desired yield, and application-specific requirements, highlighting the importance of host tailoring in industrial chitosanase production. The examples for using heterologous expression systems were mentioned in Table 2.

Table 2. Heterologous production of chitosanase isolated from different microbial sources and their activity.

Microorganism (Native Source)	Isolated Sources	Chitosanase Family	Chitosanase Name	Expression Host	Specific Activity (U/mg) *	Notable Property	Reference
Bacillus sp. *TS*	Soil	GH8	CsnTS	*E. coli*	566	-	[6]
P. barengoltzii	Marine	GH8	PbCsn8	*B. subtilis*	360.4	Bifunctional	[25]

Table 2. *Cont.*

Microorganism (Native Source)	Isolated Sources	Chitosanase Family	Chitosanase Name	Expression Host	Specific Activity (U/mg) *	Notable Property	Reference
Serratia sp. QD07	Deep-sea mud	GH46	CsnS	*E. coli*	412.6	Cold-adapted	[31]
Bacillus cereus TY24	Seafood waste	GH8	CHOE	*E. coli*	1150	-	[32]
Paenibacillus tyrfis	Peat swamp soil	GH46	OUC-CsnPT	*E. coli*	5346.56	-	[48]
Gynuella sunshinyii	Rhizosphere of a halophyte	GH46	GsCsn46A	*E. coli*	260.87	Cold-adapted	[49]
Streptomyces alblongus	-	GH46	Csn21c	*E. coli*	336.2	-	[50]
Kitasatospora setae KM-6054	Soil	GH46	CscB	*E. coli*	1094.21	Cold-adapted	[51]
Bacillus subtilis 168	-	GH46	Csn	*B. subtilis*	208.23 U/mL	-	[53]
Aspergillus fumigatus	Marine soil	GH75	Csn75	*P. pastoris*	13 U/mL	Crude Csn75 (30 U/mL); 90.65% COSs after 4 h	[55]
Bacillus amlyoliquefaciens	Seafood waste	GH46	BaCsn46B	*P. pastoris*	2380.5	-	[56]
Streptomyces griseus HUT 6037	-	GH5	Csn5	*P. pastoris*	90.62 U/mL	Crude Csn5 (20 U/mL); 91.2% COSs after 8 h	[57]
Streptomyces sp. *N174*	Soil	GH46	SsCsn46	*P. pastoris*	50,000	-	[58]
Staphylococcus capitis	-	GH46	Csn-CAP	*E. coli*	89.2	Cold-adapted	[59]
Bacillus sp. *MD-5*	-	GH46	Csn-BAC	*E. coli*	41.67	-	[60]
Paenibacillus dendritiformis	-	GH46	Csn-PD	*E. coli*	76.4	-	[61]
Amycolatopsis sp. CsO-2	Soil	GH46	CtoA	*E. coli*	88	Antifungal	[62]
Bacillus amyloliquefaciens XY-01	Fermented fruits beverages	GH46	BaCsn46A	*E. coli*	1031.2	-	[63]
Lentinula edodes	-	GH75	*Le*Cho1	*E. coli*	71.88	Acid stable	[64]
Beauveria bassiana	Insect	GH75	BbCSN-1	*P. pastoris*	101.11	Cold-adapted	[65]
Aspergillus sp. *W-2*	Soil	GH75	CsnW2	*P. pastoris*	34	-	[66]
Bacillus sp. BY01	Sea sediment	GH46	CsnB	*E. coli*	329.3	Cold-adapted	[67]
Penicillium oxalicum M2	Bird fecal	GH75	*Po*CSN75A	*P. pastoris*	2.31	-	[68]

* One unit (U) of chitosanase activity refers to the release of 1 μmol of reducing sugars (GlcN equivalents) per minute under defined assay conditions. Specific activity is reported as described in the original studies, usually in U/mg protein, though sometimes based on crude extracts.

4. Kinetics and Biochemical Properties of Chitosanases

4.1. Substrate Specificity and Product Profiles

Substrate specificity is a defining feature of chitosanases, governing their ability to recognize and hydrolyze chitosan substrates of varying molecular weights, degrees of deacetylation (DDA), and acetylation patterns. Chitosanases differ not only in their preference for fully or partially deacetylated polymers but also in their acceptance of powder or colloidal chitosan forms. In addition, product specificity of different chitosanases contributes to the diversity in COS composition and DP. These differences are rooted in the architecture of the substrate-binding cleft, the distribution of subsites, and the nature of catalytic residues, along with the hydrolysis mechanisms which form substrate recognition and influence the cleavage pattern and the degree of product polymerization [22].

Chitosanases from the GH46 family are well-known for their strict substrate specificity and endo-type cleavage patterns. The catalytic cleft formed between the upper and lower domains is a typical structural feature of GH46 family chitosanases, with conserved catalytic amino acids, including glutamic acid (Glu) and aspartic acid (Asp). In general, there are at least six sugar-binding sites −3 to +3 in the catalytic cleft, and the substrate chain is cleaved between −1 and +1 subsites by two conserved catalytic residues. The product distribution produced by chitosanases is dependent on the substrate binding at the subsites and the cleavage pattern of the enzyme [69]. The GH46 chitosanases are well characterized and produce chitobiose (GlcN)2, chitotriose (GlcN)3, and COSs with higher polymerization numbers [70].

Enzymes such as Csn-SH [71] and CsnCA [69] have demonstrated significant activity toward colloidal chitosan with high DDA from 85% to 95%, while showing negligible activity toward colloidal chitin or carboxymethylcellulose (CMC). Substrate selectivity is consistent with the conserved architecture of the GH46 active site, which accommodates GlcN-rich regions via interactions mediated by two essential catalytic residues (Glu and Asp). CsnCA exhibits a random endo-acting mechanism capable of rapidly converting colloidal chitosan into a mixture of $(GlcN)_2$ and GlcN, yet remains inactive toward chitosan powder, suggesting that enzyme–substrate interactions are not only dependent on the chemical nature (DDA) but also the physical form of the substrate. Structural insights into CsnCA revealed that $(GlcN)_3$ represents the minimal binding motif, occupying subsites −2 to +1. In addition, strong binding at the −1 subsite stabilizes the $(GlcN)_3$ in the active-site cleft, thereby directing the cleavage to generate $(GlcN)_2$ and GlcN, rather than higher oligomers or monomers. An interesting structural divergence is observed in Csn-SH, a GH46 enzyme exhibiting a substrate-binding region forming a negatively charged closed tunnel, in contrast to the open clefts commonly found in other GH46 members. This tunnel-like architecture enables Csn-SH to bind longer oligomers with $(GlcN)_5$ as the minimally recognized substrate and to hydrolyze colloidal chitosan into oligomers of DP2 to DP6. Importantly, the antifungal activity of the enzyme's hydrolysates highlights the potential of Csn-SH as a promising biocatalyst for the generation of bioactive COSs with relevance to biocontrol applications.

Chitosanases from the GH5 family exhibit a broader substrate specificity compared to GH46 and GH75 enzymes, frequently displaying bifunctional activity toward both chitosan and cellulosic substrates. For example, *Aq*CoA from *Aquabacterium* sp. A7-Y demonstrates hydrolytic activity toward highly deacetylated chitosan (DDA 95%) and carboxymethyl-cellulose (CMC-Na), indicating its broad substrate tolerance and the flexible specificity characteristic of GH5 family. *Aq*CoA cleaves chitosan into COSs with DP ranging from 3 to 5, while showing no activity toward COS substrates with DP < 6, consistent with its mode of action as an endo-acting enzyme. Structurally, *Aq*CoA adopts a canonical $(\alpha/\beta)_8$ barrel fold characteristic of GH5 enzymes, with its catalytic activity attributed to

Glu159 and Asn200 as key active-site residues. This configuration differs markedly from that of GH46 chitosanases, which typically feature Glu and Asp catalytic dyads and a more confined substrate-binding groove. The presence of a surface groove rather than a tunnel-like cleft in *Aq*CoA enables it to accommodate structurally diverse substrates. This structural flexibility is hypothesized to contribute not only to its broader substrate scope but also to its potential in producing biologically active COSs as antifungal agents for crop protection [72]. PbCsn8 [25], a GH8 chitosanase from *Paenibacillus barengoltzii*, exhibits broad substrate specificity, with the highest activity toward chitosan (388.9 U/mg for DDA 95% and 360.4 U/mg for DDA 75%), followed by barley β-glucan and lichenan, suggesting strong preference for GlcN-rich backbones. PbCsn8 comprises a GH8 catalytic domain and a C-terminal discoidin domain (DD). The open catalytic groove accommodates six GlcN units, with Glu71 and Glu258 acting as key catalytic residues. The DD enhances substrate recognition via conserved acidic residues (Glu405, Glu422, Glu426), particularly Glu405 and Glu452, which interact with the amino group of the non-reducing end GlcN. Deletion of the DD significantly reduced both chitosanase and glucanase activities, underscoring its essential role in substrate binding and degradation. The enzyme's negatively charged substrate-binding cleft likely facilitates interaction with the positively charged GlcN moieties. Product profiling revealed that PbCsn8 initially generates COSs with DP ranging from 4 to 6. Subsequent cleavage of COSs with DP 4–6 into smaller units (DP 2–3) that could hardly hydrolyze chitobiose and chitotriose, supports its endo-type mode of action. The hydrolysis property is similar to that of several GH 46 chitosanases. *Po*CSN75A exhibited strict substrate specificity, displaying significant hydrolytic activity only toward colloidal chitosan, while showing no detectable activity against powdered chitin, colloidal chitin, powdered chitosan, carboxymethyl chitosan, β-glucan, CMC-Na, or alginate. This narrow selectivity underscores the structural preference of enzyme for the physicochemical characteristics of colloidal chitosan as its natural substrate. The enzyme also demonstrated a preference for highly deacetylated chitosan, with the highest activity observed for samples with 95% degree of deacetylation. Structural modeling of *Po*CSN75A revealed key residues potentially involved in substrate binding and catalysis, including several active hydrogen bond-accepting amino acid residues (D148, D150, E159 and T149). Functionally, *Po*CSN75A operated via an endo-type cleavage mechanism, producing COS dimers and trimers as the main hydrolytic products [68].

4.2. Kinetic Parameters and Physicochemical Stability

Comprehensive kinetic evaluation of chitosanases provides critical insights into their catalytic efficiency and substrate affinity, typically expressed through the Michaelis–Menten constant (K_m), maximum reaction velocity (V_{max}), and catalytic turnover rate (k_{cat}). These parameters vary substantially not only among different GH families but also within isoforms of the same family, which reflect diverse structural adaptations and catalytic mechanisms. In parallel, physicochemical stability, including thermostability, tolerance to pH variation, and resistance to metal ions, plays a critical role in determining the functional robustness and practical applicability of chitosanases in biotechnological processes. The relationship between catalytic efficiency and physicochemical stability profiles provides a comprehensive understanding of enzyme performance, especially under industrial conditions or physiologically relevant environments. Consequently, a combined evaluation of kinetic behavior and stability features among different GH families is essential for rational enzyme selection and engineering. In this section, kinetics and biochemical properties were discussed in tandem, and key data are summarized in Table 3.

Most chitosanases from the GH46 family are characterized by an endo-type mode of action and exhibit relatively high catalytic turnover. For instance, *Sh*Csn46 from *Strepto-*

myces hygroscopicus R1 possesses a K_m of 2.1 mg/mL, V_{max} of 959 mM/min/mL, and k_{cat} of 206/min when hydrolyzing colloidal chitosan (95% DDA), indicating strong substrate affinity and efficient catalysis. With stable activity over pH 5.0–10.0 and at 40–55 °C, this enzyme is well-suited for various processing applications [73]. Similarly, *Streptomyces* chitosanases, such as those from strains N174 (CsnN174) [74] (K_m = 26.1 μg/mL; k_{cat} = 642.1/min) and *SirexAA-E* [75] (K_m = 2.2 mg/mL; k_{cat} = 11.2/s) highlight the kinetic diversity within the GH46 family, even among members of the same genus.

However, elevated catalytic activity does not always correlate with thermal stability. For example, Sn1-CSN from *S. niveus* retains activity at extreme pH values (pH 4.0–11.0) but rapidly loses activity above 45 °C [76]. In contrast, Csn21c from *S. albolongus* [50] demonstrates both thermostability (35–55 °C) and a unique alkaline optimum (pH 8.0) compared with other *Streptomyces* chitosanases that are commonly acidic optimum. This divergence underscores the necessity for pH optimization or substrate pre-conditioning in specific process designs because acidic conditions are generally favorable for chitosan hydrolysis to improve polymer solubility. Interestingly, the catalytic enhancement or inhibition by metal ions also reveals divergent active-site architectures. While chitosanases such as *Sh*Csn46 (*S. hygroscopicus*) [73] and SaCsn46A (*S. avermitilis*) [77] are activated by Mg^{2+} but inhibited by Cu^{2+}, Sn1-CSN [76] uniquely displays enhanced activity in the presence of Cu^{2+}, suggesting unique metal-ion interaction profiles linked to active-site architecture. Of particular interest are cold-adapted chitosanases such as CscB from *Kitasatospora setae* KM-6054 [51] and GsCsn46A from *Gynuella sunshinyii* [49] exemplify the functional versatility of the GH46 family. Both exhibit optimal activity at 30 °C. These enzymes display effective catalytic profiles (K_m 4.39 mg/mL and V_{max} 555.56 μmol/mg/min for CscB; K_m 1.97 mg/mL and V_{max} 385.65 μmol/mg/min for GsCsn46A), indicating that efficient catalysis is not restricted to thermophilic enzymes. Their cold-active profiles may benefit bioconversion processes under energy-saving or temperature-sensitive conditions such as in food-grade oligosaccharide production. For GH75 chitosanases, primarily from fungal sources, show complementary kinetic and biochemical profile. In a study performed by Zhou et al. [55] Csn75 from *Aspergillus fumigatus* CJ22-326 exhibited strong substrate affinity (K_m = 0.46 mg/mL) and high catalytic efficiency (V_{max} = 6.03 μmol/mL/min) with optimal activity at 55–65 °C and pH 5.0–6.0. Its catalytic capacity was significantly enhanced (~4-fold) by Mn^{2+}, and the resulting COS products demonstrated antifungal effects against phytopathogens, indicating potential use in biocontrol applications. Similarly, *Po*CSN75A from *Penicillium oxalicum* M2 exhibits favorable kinetic parameters, with a low K_m of 0.27 mg/mL and a V_{max} of 4.36 U/mL, reflecting high substrate affinity toward chitosan with a 95% DDA. The enzyme remains active under acidic conditions (pH 3.0–6.0) and stable at temperatures up to 45 °C. In addition, the presence of divalent metal ions such as Ca^{2+} and Mn^{2+} significantly enhances its catalytic efficiency. These findings contribute to the expanding understanding of GH75 chitosanases and provide valuable data supporting their potential use in environmentally friendly COS production [68]. In contrast, CsnW2 from *Aspergillus* sp. W-2 remains functionally stable across pH values from 3.0 to 10.0 and temperatures ranging from 30 to 70 °C. Although its catalytic efficiency is relatively low (K_m = 7.10 mg/mL; k_{cat} = 0.47/s), the activity of CsnW2 is significantly enhanced in the presence of Ca^{2+}, Mn^{2+}, and Mg^{2+}. The enzyme displays substrate specificity toward chitosan and shows a preference for highly deacetylated forms. These characteristics highlight its potential for industrial applications under variable processing conditions [66]. For GH8 and GH5 chitosanases, kinetic performance and physicochemical resilience vary significantly depending on bacterial origin and structural configuration, offering complementary characteristics to those observed in GH46 and GH75 families. The GH5 chitosanase Csn5 from *Streptomyces griseus* HUT 6037 exhibits a favorable kinetic profile (V_{max} of

42.55 μmol/mL/min and K_m of 0.91 mg/mL) with optimal performance at 55 °C and pH 5.5–6. Notably, Csn5 also possesses transglycosylation activity, which suggests a dual functionality advantageous for generating COSs with tailored polymerization patterns. While Cu^{2+} functions as an inhibitor, Mn^{2+} significantly enhances enzymatic activity. This contrasting effect reflects the differential interactions of metal ions with active-site residues, which may be influenced by the structural stabilization conferred by internal disulfide linkages. The COS products generated by the enzymatic activity of Csn5 exhibited notable antioxidant capacity. This property highlights the enzyme's potential for producing bioactive oligosaccharides applicable in food safety and health-related fields [57]. In contrast, the GH8 chitosanase CHOE from *Bacillus cereus* TY24 demonstrates a remarkably high catalytic rate with V_{max} and K_m values of 1401.9 μmol/min/mg and 3.03 mg/mL, respectively [32]. Although the higher Km denotes reduced substrate affinity relative to Csn5, the substantial catalytic rate makes CHOE a strong candidate for high-throughput bioconversion. CHOE exhibited strong thermal and pH stability, with more than 80% of its activity maintained across pH 4.5–7.5 and at temperatures between 30 °C and 65 °C. Interestingly, CHOE activity increased markedly in the presence of various metal ions, including Mn^{2+}, Mg^{2+}, K^+, and notably Cu^{2+}, which increased activity to 153%. This positive Cu^{2+} effect is exceptional given its inhibitory role in other chitosanases such as Sn1-CSN (GH46), Csn5 (GH5), implying a distinctive metal-ion binding profile at the active site that may enhance catalytic turnover.

Overall, these data demonstrate that while each GH family offers distinct advantages in terms of catalytic parameters and physicochemical stability, the interplay of metal ion sensitivity, temperature and pH preferences, and transglycosylation capability ultimately dictates their suitability for specific applications. Understanding these biochemical profiles not only supports rational enzyme selection but also guides strategies for performance enhancement.

Despite the inherent diversity in natural chitosanase kinetics and stability, further enhancement of these properties is often required to meet the stringent demands of industrial bioprocessing. In this context, advances in protein engineering and computational design have enabled the development of tailored chitosanase variants with improved performance, substrate scope, and environmental adaptability. The following section explores the recent progression of in silico modeling, rational mutagenesis, and directed evolution as tools to optimize chitosanase efficiency and stability across application domains.

Table 3. Kinetic parameters and physiochemical stability of chitosanases isolated from different microbial sources.

Microorganism	Chitosanase Name	*V*max	*K*cat	*K*m	Optimal Temp. (°C)	Optimal pH	Metal Ions (+)	Metal Ions (−)	Substrate Specificity	End Prodcuts	Reference
Bacillus amyloliquefaciens	*Bam*Csn	-	2.04×10^2/s	0.587 mg/mL	40	5.6	-	-	90% DDA	DP > 3	[7]
Bacillus paramycoides BP-N07	*Bp*CSN	2727.03 μM/min/mg	-	4.063 mg/mL	50	6	Mn^{2+}	Fe^{3+}, Ag^{2+}, Hg^{2+}	Chitosan	DP 2–4	[30]
Bacillus cereus TY24	CHOE	1401.9 μM/min/mg	-	3.03 mg/mL	65	5.5	Mn^{2}, Cu^{2+}, Mg^{2}, K^{+}, Ca^{2+}	Zn^{2+}, Co^{2+}, Al^{3+}, Hg^{2+}, Pb^{2+}, Fe^{3+}	colloid chitosan	-	[32]
Gynuella sunshinyii	GsCsn46A	385.65 μM/min mg	-	1.97 mg/mL	30	5.5	-	-	-	DP 2–7	[49]
Streptomyces albolongus ATCC 27414	Csn21c	263.1 μM/min/mg	-	7.4 mg/mL	35–55	8	Mn^{2+}	Fe^{3+}	>90%DDA	DP 1–3	[50]
Kitasatospora setae KM-6054	CscB	555.56 μM/mg/min	-	4.389 mg/mL	30	6	Na^{+}, K^{+}, Ca^{2+}, Mg^{2+}	Fe^{3+}, Cu^{2+}, Ni^{+}, Co^{2+}, Zn^{2+}	-	DP 2–4	[51]
Aspergillus fumigatus CJ22-326	Csn75	6.03 μM/mL/min	-	0.46 mg/mL	55–65	5.0–6.0	Mn^{2+}, Co^{2+}, Fe^{2+}, Ca^{2+}	Mg^{2+}, Cu^{2+}	-	DP 2–6	[55]
Streptomyces griseus HUT 6037	Csn5	42.55 μM/mL/min	-	0.91 mg/mL	55	5.5–6.0	Ca^{2+}, Mn^{2+}	Mg^{2+}, Fe^{2+}, Cu^{2+}, Co^{2+}, Na^{+}	DDA ≥ 95%	DP 2–4	[57]
Bacillus amyloliquefaciens	BaCsn46A	7142.9 μM/min/mg	-	2.8 mg/mL	50	6	-	-	DDA ≥ 95%	DP 2–3	[63]
Lentinula edodes	*Le*Cho1	76.81 μM/min/mg	-	0.04 μM	50	3	Mn^{2+}	Fe^{3+}	95% DDA	DP 2–5	[64]
Beauveria bassiana	BbCSN-1	3.9 g/min	-	0.8 mg/mL	30	5	Mn^{2+}	Co^{2+}, Cu^{2+}	colloidal chitosan	DP 2–3	[65]

Table 3. *Cont.*

Microorganism	Chitosanase Name	*V*max	*K*cat	*K*m	Optimal Temp. (°C)	pH	Metal Ions (+)	Metal Ions (−)	Substrate Specificity	End Prodcuts	Reference
Aspergillus sp. *W-2*	CsnW2	1.58 mM/L/min	0.47/s	7.10 mg/mL	55	6	Ca^{2+}, Mn^{2+}, Mg^{2+}	Fe^{2+}, Zn^{2+}, Ge^{2+}, Ni^{2+}, Cu^{2+}	92%DDA	DP 2–6	[66]
Penicillium oxalicum M2	*Po*CSN75A	4.36 U/mL	-	0.27 mg/mL	60	5.5	Ca^{2+}, Mn^{2+}	Cu^{2+}, Zn^{2+}, Mg^{2+}, Fe^{2+}, Ba^{2+}	95% DDA	DP 2–3	[68]
Bacillus atrophaeus BSS	Csn-SH	140.05 mM/mg/min	-	0.50 mg/mL	45	5	Mn^{2+}	Cu^{2+}, Zn^{2+}, Fe^{2+}, Al^{2+}	DDA≥95%	DP 2–4	[71]
Streptomyces hygroscopicus R1	*Sh*Csn46	959 mM/min/mL	206/min	2.1 mg/mL	55	5.5	Mn^{2+}	Cu^{2+}, Fe^{2+}, Al^{3+}	95% DDA	DP 2–6	[73]
Streptomyces sp. *N174*	CsnN174	-	642.1/min	26.1 μg/mL	-	5.5	-	-	97% DDA		[74]
Streptomyces sp. *SirexAA-E*	SACTE_5457	25 mM/mg/min	11.2/s	2.2 mg/mL	45	6	-	-	>90% DDA	DP 2–7	[75]
Streptomyces avermitilis	SaCsn46A	526.32 U/mg/min	-	1.32 mg/mL	45	6.2	Mn^{2+}	Cu^{2+}, Ba^{2+}, Ca^{2+}, Zn^{2+}	colloidal chitosan	DP 1–2	[77]
Bacillus sp. TS	-	674.71 μM/min	5.05×10^5/s	1.19 mg/mL	60	5	Mn^{2+}	Co^{2+}, Hg^{2+}, Cu^{2+}	>90%DDA	DP 3–6	[78]
Streptomyces lydicus S1	SlCsn46	1375.7 mM/min/mL	-	1.92 mg/mL	50	6	Mn^{2+}	Al^{3+}, Cu^{2+}	95% DDA	DP 2–6	[79]
Bacillus thuringiensis B-387	-	43 μM/mL/min	4.79×10^4/s	0.22 mg/mL	55	6.5	Mg^{2+}, Mn^{2+}	Hg^{+}, Cd^{2+}, Zn^{2+}, Ag^{+}	85%DDA	DP 2–5	[80]
Bacillus mojavensis SY1	CsnBm	2802 mM/min/mg	-	0.71 mg/mL	55	5.5	Ca^{2+}, Zn^{2+}, Mg^{2+}, Mn^{2+}	Fe^{2+}, Cu^{2+}	90%DDA	DP 2–6	[81]
B. mojavensis EGE-B-5.2i	-	244.5 μM/min/mg	7.53×10^2/s	2.1 mg/mL	55	5.5	Mn^{2+}, K^{+}	Hg^{2+}, Cu^{2+}	-	DP 2–6	[82]

5. Protein Engineering and In Silico Design of Chitosanases

Advancing the functional versatility of chitosanases is essential to unlock their full potential in industrial biocatalysis, biomedical formulations, and green bioprocessing. Because wild-type chitosanases exhibit unstable properties under application-specific conditions [83,84], protein engineering has become a central strategy for tailoring their properties. Two complementary approaches have emerged including experimental engineering, which involves direct sequence manipulation and screening of enzyme variants; and computational redesign, which uses structure-based modeling and simulations to support and refine rational modifications. Combined, these approaches form a comprehensive platform for enhancing chitosanase function from molecular design to practical applications. Representative mutational and computational strategies for enhancing chitosanase performance are shown in Table 4.

Table 4. Representative mutational and computational strategies for enhancing chitosanase performance.

Enzyme	Mutation(s)	Engineering Strategy	Targeted Property	Observed Improvement	Reference
*Bc*Cn8A (*Bacillus cereus* GX-90)	*Bc*Cn8A-ΔN4-V319L	Site-directed mutagenesis	Catalytic efficiency Thermal stability	310% increase in specific activity, retained 93.2% activity at 50 °C vs. 42.1% (WT), over 60% of its activity across the 50–70 °C	[5]
CsnTS (*Bacillus* sp. TS)	S265G, S276A and S347G	Site-directed mutagenesis	Thermostability	$t_{1/2}$ at 60 °C increased from 5.32 min to 34.57 (S265G), 36.79 (S276A), 7.2 (S347G) min	[6]
BsCsn46A (*Bacillus subtilis*)	P121N, P121C, P121V	Site-saturation mutagenesis	Catalytic efficiency	Specific activity increased up to 1.69-, 1.97-, and 2.15-fold for P121N, P121C, and P121V, respectively, no loss of thermostability in P121N	[8]
Csn46 (*Bacillus amyloliquefaciens* KCP2)	Mut4 (A129L/T175V/K70T/D34G)	Site-directed mutagenesis	Catalytic efficiency Thermal stability Product profile	Specific activity increased from 1671.73 to 3528.77 U/mg $t_{1/2}$ at 60 °C increased from 34.31 to 690.80 min expanded product range (DP 2–7) at 70 °C	[9]
Csn-PD (*Paenibacillus dendritiformis*)	Csn-PDT6 (I101M/T120E/T220G)	Site-directed mutagenesis	Catalytic efficiency pH stability	8-fold increase in catalytic activity compared to the WT, Csn-PD was stable only at pH 6–7, while Csn-PDT6 retained >66% relative activity after incubation at pH 4–9	[10]
SaCsn46A (*Streptomyces avermitilis*)	TJA	Site-directed mutagenesis	Product profile	Shifted product ratio (chitobiose: chitotriose) from 1:1 to 15:7	[11]
CsnMY002 (*Bacillus subtilis*)	Mut6	Site-directed mutagenesis	Thermal stability	$t_{1/2}$ value at 55 °C and 75 °C increased by 1.80 and 1.62 times, respectively compared with WT	[14]
	Mut2		Catalytic efficiency	1.52 times increase in catalytic efficiency compared to WT	[14]

Table 4. *Cont.*

Enzyme	Mutation(s)	Engineering Strategy	Targeted Property	Observed Improvement	Reference
SsCsn46 (*Streptomyces* sp. N174)	m-SsCsn46	Site-directed mutagenesis	Product profile	Shifted hydrolysis product from COSs (DP 3–5) to mainly chitopentasaccharide (DP5)	[58]
CsnMY002 (*Bacillus subtilis*)	G21 K	Site-saturation mutagenesis	Product profile	~87% of chitobiose for G21 K mutant, ~57% of that for the WT	[70]
OUC-CsnA4 (*Methanosarcina* sp. 1.H.T.1A.1)	S49I and S49P	Site-saturation mutagenesis	Product specificity	Enabled production of $(GlcN)_5$ (up to 24% for S49I, 26% for S49P); WT produced no detectable $(GlcN)_5$	[85]
BaCsn46A (*Bacillus amyloliquefaciens*)	S196A	Site-saturation mutagenesis	Catalytic efficiency Thermal stability	Specific activity increased by 118.79%, remained above 80% at 60 °C	[86]
CsnMY002 (*Bacillus subtilis*)	G21R and G21K	Molecular dynamics simulations	Product profile DP diversity of COSs	Increased COS yield; altered substrate binding and catalytic modes → greater DP variation in products	[87]
BsCsn46A (*Bacillus subtilis*)	K242P	Site-saturation mutagenesis	Catalytic efficiency Thermal stability	The catalytic activity of K242P increased from 12,971 ± 597 U/mg of wild type to 17,820 ± 344 U/mg, and the thermostability of K242P increased by 2.27%	[88]

5.1. Engineering Strategies for Functional Enhancement of Chitosanases

Experimental protein engineering has played a crucial role in enhancing the functional properties of chitosanases to meet the demands of industrial and biomedical applications. Through approaches such as directed evolution, rational design, and semi-rational design, researchers have significantly improved catalytic efficiency, thermal and pH stability, substrate specificity, and expression levels. These strategies involve systematic sequence modifications followed by iterative functional screening and biochemical evaluation. This section summarizes key experimental approaches used to tailor chitosanases and highlights representative studies demonstrating their practical effectiveness.

A recent study on the GH8 family chitosanase *Bc*Cn8A demonstrated the critical influence of the conserved N-terminal region on catalytic activity and substrate binding. Truncation mutagenesis revealed that this region exerts a negative regulatory effect by disrupting substrate recognition and transport within the catalytic tunnel. Guided by evolutionary analysis and computational modeling, a focused mutational strategy was employed to modify selected residues within this region and at distal positions. This led to the generation of the optimized variant *Bc*Cn8A-ΔN4-V319L, which exhibited a remarkable 310% increase in specific activity and a 5 °C improvement in optimal temperature. In addition, *Bc*Cn8A-ΔN4-V319L retained 93.2% and 86.7% activity at 50 °C and 55 °C, respectively, outperforming the wild type, which retained only 42.1% at 50 °C. Furthermore, the engineered enzyme efficiently produced COSs with DP ranging from 2 to 7 with both antioxidant and anti-browning properties. These findings highlight that the generated mutant simultaneously improved catalytic efficiency and thermostability and position it as a highly promising enzyme candidate for industrial-scale COS production and food preservation [5]. Another approach conducted by Wu et al. [9], a structure-guided rational design strategy was employed to improve the thermostability and catalytic efficiency of the GH46 chitosanase Csn46 from *Bacillus amyloliquefaciens* KCP2. Four single-point mutations

(A129L, T175V, K70T, and D34G), each individually predicted to enhance enzyme stability, were rationally combined to generate a multi-site mutant, designated Mut4. Among these, the D34 substitution played a pivotal role in modifying the microenvironment of the substrate-binding pocket. The removal of the charged aspartic acid side chain at the pocket entrance reduced steric hindrance, thereby facilitating chitosan access and improving both thermal resilience and catalytic turnover. The resulting variant, Mut4, demonstrated a substantial enhancement in thermostability, with its half-life at 60 °C increasing from 34.31 to 690.80 min. Additionally, its specific activity was elevated from 1671.73 to 3528.77 U/mg. Notably, Mut4 retained strong catalytic activity at elevated temperatures, efficiently producing COSs with DP 2–4 at 60 °C and DP 2–7 at 70 °C. These results indicate the efficacy of rationally guided combinatorial mutagenesis in fine-tuning chitosanase properties for industrial-scale, high-temperature bioconversion processes. In the case of *Bacillus subtilis* chitosanase BsCsn46A, Pro121 was identified as a structurally atypical residue that did not conform to the α-helical configuration in its region, situated on the side opposite the active center. To investigate its functional role, site-saturation mutagenesis was performed at position 121. Among the resulting variants, the P121N mutant exhibited a 1.69-fold increase in specific activity on colloidal chitosan while largely retaining thermostability. In addition, P121N mutant also displayed a decrease in optimal temperature from 60 °C to 55 °C. These findings highlight the critical influence of Pro121 on the conformational flexibility and catalytic efficiency of BsCsn46A and suggest that relieving architectural constraint at this site can significantly enhance enzymatic activity. This approach offers a promising strategy for engineering chitosanases suitable for COS production under milder processing conditions [8]. Given the growing interest in COSs with higher DP (4–6), which exhibit superior bioactivities in functional food and pharmaceutical applications compared to their lower-DP counterparts (DP 1–3), enhancing chitosanase specificity for high-DP COSs (HdpCOSs) has emerged as a desirable engineering objective. A structure-guided strategy was applied to the GH46 chitosanase OUC-CsnA4 from *Methanosarcina* sp. 1.H.T.1A.1, which focuses on subsite interactions that influence product profiles. Structural modeling and analysis of enzyme–substrate interactions identified Ser49, positioned near a critical subsite in the catalytic cleft, as a modifiable residue affecting substrate binding and product specificity. Site-directed mutagenesis at Ser49 yielded two variants, S49I and S49P, which significantly altered the product distribution. These engineered enzymes produced $(GlcN)_5$ at yields of 24% and 26%, respectively, whereas the wild-type enzyme did not produce detectable levels of this oligomer. The substitutions also shifted substrate binding preferences toward longer-chain substrates (DP > 5) and thereby supported enhanced HdpCOS production. These findings emphasize the importance of substrate positioning at the reducing end and highlight Ser49 as a key engineering target for modulating product specificity in chitosanases designed for targeted oligosaccharide production [85]. Fusion of a carbohydrate-binding module (CBM) has emerged as an effective protein engineering strategy to enhance chitosanase performance. Zhou et al. applied this approach to Csn75, a GH75 chitosanase from *Aspergillus fumigatus* CJ22-326, by fusing it with one or two copies of a CBM32 domain at the C-terminus to generate the variants Csn75-CBM32 and Csn75-2CBM32. Csn75-CBM32 exhibited a substantial enhancement in enzymatic function, with specific activity increased by 59.2% relative to the wild-type enzyme. Thermal stability was also improved, as evidenced by an 18.34% increase in the residual activity of Csn75-CBM32 (88.45%) at 50 °C for 2 h, and a higher melting temperature (Tm) of 53.69 °C compared to 49.44 °C for the native enzyme. Thermodynamic analysis indicated that these improvements were associated with enhanced substrate binding, primarily driven by favorable enthalpic contributions, in contrast to the hydrophobic binding of the native enzyme. In addition, Csn75-CBM32 expanded the product profile toward COSs

with higher DP (3–5), whereas the wild-type enzyme predominantly produced DP 2–4. This shift underscores the role of CBM in modulating both binding affinity and product specificity. Although the addition of a second CBM32 domain (Csn75-2CBM32) further elevated thermostability, with 90.63% residual activity and a melting temperature (Tm) of 55.24 °C, the improvement in catalytic activity was less significant at 14.3%. The result indicates that CBM copy number must be carefully optimized to minimize potential steric or conformational drawbacks. Overall, CBM fusion represents a promising and modular strategy to simultaneously enhance chitosanase activity, stability, and product selectivity for industrial applications [89]. GH46 chitosanase Csn-PD from *Paenibacillus dendritiformis*, an enzyme that predominantly produces chitobiose $(GlcN)_2$. Based on structural insights, four residues (I101, T120, T220, and Y259) were selected for targeted mutagenesis. Subsequent site-directed mutagenesis and combinatorial screening led to the construction of a triple mutant, Csn-PDT6 (I101M/T120E/T220G), which demonstrated an eightfold increase in catalytic activity compared to the wild-type enzyme. Additionally, Csn-PD was stable only at pH 6–7, whereas Csn-PDT6 retained over 66% relative activity at pH 4–9, broadening its applicability under varying process conditions. The hydrolysis products generated by Csn-PDT6 remained highly specific, with $(GlcN)_2$ as the major product, underscoring its utility for the production of high-purity COSs. Structural analysis of the mutant enzyme suggested that the enhanced activity was attributable to reconfigured hydrogen bonding and electrostatic interactions within the catalytic site, along with the alleviation of unfavorable steric constraints. These findings highlight the effectiveness of semi-rational design in refining both catalytic efficiency and stability while maintaining desirable product specificity, offering a generalizable strategy for the functional optimization of chitosanases [10]. Site-saturation mutagenesis at S196 was studied by Jing et al. for improving catalytic activity and thermostability of BaCsn46A [86]. The amino acid residue Ser196, positioned adjacent to the catalytic center of *Bacillus amyloliquefaciens* chitosanase BaCsn46A, was identified as a critical determinant of both enzymatic activity and thermostability. To investigate its functional role, site-saturation mutagenesis at position 196 was performed. Among the generated variants, the S196A mutant exhibited a 118.79% increase in specific activity and significantly improved thermostability compared to the wild-type enzyme. In contrast, substitution with proline (S196P) resulted in a drastic loss of activity, retaining only 2.41% of the wild-type level, highlighting the sensitivity of this position to side-chain structure and flexibility. Notably, no significant alterations in secondary structure between the wild-type and mutant enzymes were observed by circular dichroism (CD) spectroscopy. This finding suggests that the observed improvements in enzymatic properties were attributed to local changes in residue interactions rather than global conformational rearrangements. This study underscores the importance of residue 196 in fine-tuning the functional attributes of BaCsn46A and provides a rational basis for engineering robust chitosanases with improved catalytic efficiency and thermostability for industrial applications.

Despite these advances, current engineering strategies for chitosanases still face several challenges. Directed evolution requires extensive screening efforts, while rational and semi-rational design approaches remain limited by incomplete understanding of structure–function relationships, often resulting in trade-offs between activity, stability, and product specificity. Moreover, most engineered variants are optimized under laboratory conditions, which may not reflect industrial settings and thus limit scalability and robustness. These limitations highlight the need for integrated strategies combining computational prediction with experimental validation to generate application-oriented chitosanases.

5.2. Computational Redesign and Molecular Dynamics

Complementing experimental strategies, computational tools now offer powerful means to guide chitosanase engineering with higher precision and reduced experimental workload. Structure prediction, molecular docking, and molecular dynamics simulations provide atomistic insights into enzyme–substrate interactions, conformational flexibility, and the energetic effects of mutations. These in silico approaches facilitate the identification of mutation-prone regions, optimization of active sites, and prediction of enzyme performance under different environmental conditions. This section highlights recent advances in computational modeling and simulation techniques applied to the rational design and functional refinement of chitosanases.

An in-depth computational study was conducted to elucidate the functional role of the non-conserved residue Thr22, located adjacent to the catalytic Glu19 in a *Bacillus subtilis*-derived chitosanase. Bioinformatics analysis first highlighted Thr22 as a potentially important site. Site-directed mutagenesis replacing Thr22 with proline (T22P) revealed significant changes in both catalytic activity and thermostability. Molecular docking demonstrated that the T22P–substrate complex formed fewer interactions than the wild type (WT), notably lacking contacts with three catalytically essential residues. This reduction in binding interactions was attributed to the structural rigidity introduced by the proline substitution, which likely impaired substrate accommodation. Consistently, the higher binding energy of T22P (107.10 kcal/mol) relative to the wild-type enzyme (−91.44 kcal/mol) aligns with its reduced enzymatic activity. Molecular dynamics (MD) simulations were further employed at 313 K and 328 K to evaluate conformational flexibility. Root mean square fluctuation (RMSF) analysis revealed similar overall trends between WT and T22P; however, increased flexibility was noted in specific regions (residues 22–23 and 147–151) in the T22P mutant, which are implicated in shaping the catalytic pocket. Root mean square deviation (RMSD) profiles showed that the T22P mutant had lower structural deviations at 313 K compared to WT. This observation points to an improvement in structural stability at moderate temperature. At 328 K, RMSD values of T22P and WT were comparable, but T22P showed slightly reduced atomic displacement. These findings imply that although the T22P mutation compromises substrate binding and catalytic efficiency, it contributes to enhanced thermal stability. The study underscores the influence of non-conserved residues near the catalytic core on chitosanase function and stability and demonstrates how integrative use of docking and MD simulations can guide rational enzyme redesign [90]. A representative study explored the role of a conserved Glu160 residue in the thermostability of GH46 chitosanase CsnA. Sequence alignment, structural analysis, and MD simulations revealed that Glu160 forms a hydrogen-bond network with Lys163 and Thr114, which contributes to the stabilization of the relative positioning between the two catalytic lobes. Four mutants (E160A, E160Q, K163A, and T114A) which partially or completely destroy this network were constructed to prove functional significance. MD simulations showed that all variants maintained global structural stability (RMSD), but disruption of the Glu160-centered network particularly via side-chain shortening led to notable fluctuations in inter-lobal distance (Asp86–Met241), indicating increased conformational flexibility. Correspondingly, the loss of this network significantly decreased thermostability. These results highlight how MD-informed mutational analysis can uncover key stabilizing interactions and inform rational strategies for enhancing enzyme robustness [91]. To elucidate the structural basis underlying the improved catalytic performance of the engineered Csn-PDT6 variant, molecular docking simulations were performed using Discovery Studio 4.5, focusing on the interaction between the enzyme and the hexameric substrate $(GlcN)_6$. The docking results revealed that both the wild-type Csn-PD and the mutant Csn-PDT6 engage $(GlcN)_6$ via a conserved set of 14 catalytic cleft residues, including Pro76, Glu77, Arg97, Asp113, His115,

Pro116, Asp117, Asn216, Gln217, Gly218, Gly220, Tyr259, Asn260, and Met298. Despite the conservation of these contact residues, the mutant enzyme exhibited enhanced binding interactions, forming 16 hydrogen bonds with $(GlcN)_6$, compared to 15 hydrogen bonds formed by the wild type. Furthermore, 10 residues in the Csn-PDT6 mutant contributed to these hydrogen bonds, versus 11 residues in the wild type. This difference reflects redistribution of interaction networks rather than a simple increase in contact points. The strengthened hydrogen-bonding network, together with reduced unfavorable interactions and the emergence of additional favorable ionic contacts, likely contributes to the improved activity and lower Km value of Csn-PDT6 compared to the wild type [10]. Chitosanase *Bam*Csn from *Bacillus amyloliquefaciens* is an endo-acting chitosanase and generated longer-chain-length COSs from chitosan. It also cleaved chitin oligosaccharides and showed TG on chitotetraose and chitopentaose. To investigate the structural determinants of catalytic activity in *Bam*Csn, six site-directed mutants (E19A, E31A, D35G, T40H, Y118S, and W204A) were generated. Notably, the W204 mutation, which targeted a non-conserved tryptophan residue, resulted in complete loss of enzymatic activity and highlighted its essential role in active-site organization. Molecular docking using a homology model of *Bam*Csn revealed that chitosan hexasaccharide binds across the –3 to +3 subsites with key contributions from hydrogen bonds and alkyl–π interactions. Comparative structural analysis with other GH46 chitosanases showed that W204 is uniquely located in a loop projecting into the binding cleft in *Bam*Csn, whereas in class I and III homologs the analogous region lacks this residue or buries it within the protein core. These findings suggest that W204 contributes to a unique substrate-recognition mode in *Bam*Csn. This study demonstrates that computational modeling and structural comparison can identify non-conserved yet functionally essential residues and serve as effective tools for rational enzyme redesign [7]. A variety of computational methods have been developed to predict potential mutations that could enhance chitosanase stability and activity, offering mechanistic insights into how structural fluctuations and intramolecular interactions influence enzyme performance under thermal and catalytic stress [92]. A comprehensive design strategy based on insights into the enzyme structure–property relationship was performed to improve the enzymatic properties of the chitosanase CsnMY002 from *Bacillus subtilis* using residue-folding free energy changes combined with the consensus sequence analysis. The root mean square deviations (RMSDs), root mean square fluctuations (RMSFs), radius of gyration (Rg), solvent-accessible surface area (SASA), hydrogen bonding number, surface area, volume of substrate cavity, dynamical cross-correlation analysis, folding free energy (ΔG), and consensus sequence analysis were performed between the wild type and variants. Guided by the simulation results, a synergistic strategy was employed to adjust the rigidity of local structures, resulting in 50% beneficial substitutions among the screened single-point mutations. Among them, Mut6 (A49G/K70A/S84A/N89G/D199R/N221G) was obtained with significant improvement in thermal stability, with T_m and T_{50} values elevated by 3 °C and 10 °C, respectively, and a prolonged half-life ($t_1/_2$) of 209 min at 55 °C, which was 1.8 times longer than that of the wild-type enzyme. In addition, Mut2 displayed superior catalytic activity and retained thermal stability comparable to the wild type. MD simulations and structural analysis indicated that reducing fluctuations of the surface flexible regions to maintain homeostasis in the catalytic core was key to improving the thermostability of CsnMY002, and appropriately increasing the internal catalytic regions flexibility might improve catalytic efficiency. This work provided two modified mutants excellent biocatalyst with potential commercial value for the industrial production of COSs. These results should give referable guidelines for improving the properties of other enzymes [14].

6. Bioprocess Optimization and Green Production Approaches

Following advances in our understanding of chitosanase structure, catalytic mechanisms, microbial origin, and engineering strategies, increasing attention has been directed toward the development of sustainable and economically viable production methods. Bioprocess optimization not only ensures higher yields and functional stability of chitosanases but also conforms to green chemistry principles by minimizing environmental impact. This section highlights recent progress in utilizing cost-effective fermentation strategies and advanced catalyst systems to improve chitosanase production efficiency and applicability in industrial biocatalytic processes. A schematic representation of chitosanase green production approach is presented in Figure 3.

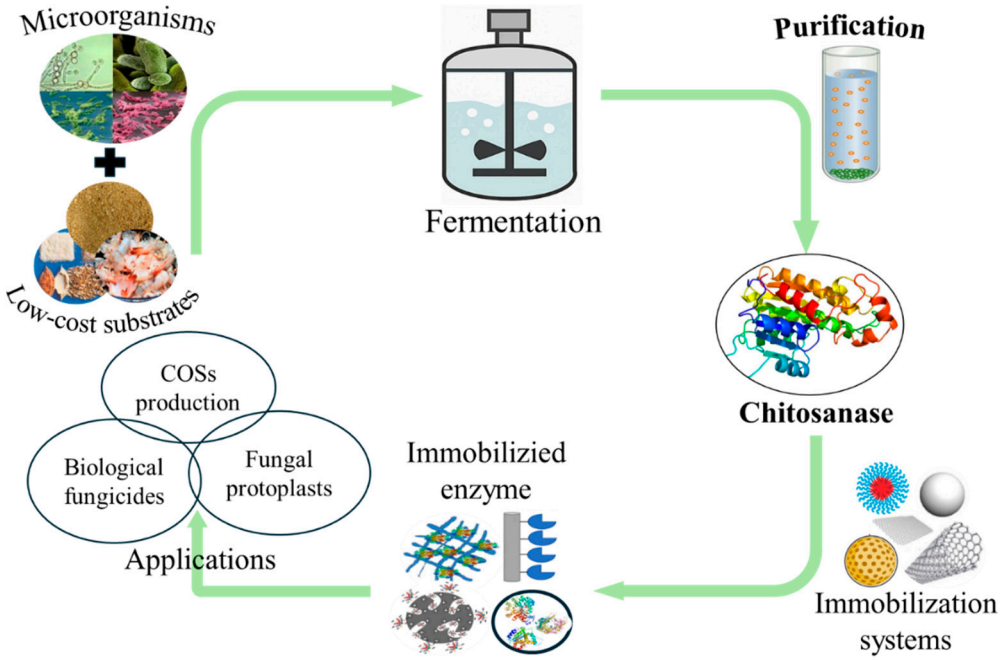

Figure 3. A schematic representation of chitosanase green production approach.

6.1. Fermentation Using Low-Cost Substrates

The selection of suitable substrates for microbial fermentation plays a pivotal role in lowering production costs and enhancing the scalability of chitosanase-based bioprocesses. Conventional carbon and nitrogen sources are often associated with economic and environmental challenges for large-scale applications. Therefore, the use of agro-industrial residues, seafood byproducts, and other low-cost materials has gained attention as sustainable alternatives to support microbial growth and enzyme induction [93]. An overview of recent developments in substrate selection and optimization strategies that facilitate efficient chitosanase production while adhering to circular bioeconomy principles.

Among various microbial systems explored for low-cost enzyme production, *Paenibacillus mucilaginosus* TKU032 demonstrated high chitosanase activity when cultivated in a medium containing shrimp head, as the sole carbon/nitrogen source. The chitosanase produced under these conditions exhibited favorable catalytic characteristics. It showed an optimal temperature and maintained thermal stability up to 70 °C, which demonstrates its potential for industrial applications. Moreover, COS fractions generated through the hydrolysis of colloidal chitosan by TKU032-derived chitosanase displayed significant α-glucosidase inhibitory and antioxidant activities. These properties support their potential utility in medical and nutraceutical applications [34]. Similarly, *Paenibacillus* sp. TKU047 was evaluated for its ability to produce chitosanase on various fishery processing residues.

Among the tested substrates, 2% (w/v) squid pen powder yielded the highest enzyme activity, serving as the sole carbon and nitrogen source. The enzyme exhibited optimal activity at 60 °C and pH 7 with enhanced catalytic efficiency toward highly deacetylated chitosan substrates. Hydrolysis of 98% DDA chitosan using TKU047-derived chitosanase resulted in chitooligosaccharide (COS) products with DP ranging from 2 to 9, consistent with an endo-type cleavage mechanism. Notably, the resulting COSs demonstrated superior DPPH radical scavenging activity compared to commercial COSs, with a maximum activity of 81.20% and an IC_{50} value of 1.02 mg/mL. In addition to antioxidant effects, the production of high-DP COSs is particularly interest due to their well-documented antimicrobial and antitumor activities, which have been reported to manifest predominantly in COSs with DP greater than 5 [94,95]. Moreover, COSs within the DP range of 4–6 have demonstrated healing and anti-inflammatory properties, supporting their potential applications in pharmaceutical formulations [96–98]. These findings collectively highlight the dual value of the TKU047 system, not only as a low-cost approach for enzyme production, but also as an effective strategy for generating high-value COSs with therapeutic potential. Despite the diverse studies on microbial chitosanase production, data on the statistical optimization of enzyme synthesis using low-cost substrates remain limited. For instance, *Paenibacillus elgii* TKU051 cultivation on squid pens as the sole carbon/nitrogen source demonstrated a 2.6-fold enhancement in chitosanase activity, reaching 2.023 U/mL upon fermentation optimization compared to the unoptimized medium. The enzyme exhibited maximal activity at pH 5.5 and maintained stability between pH 5.0 and 9.0, with optimal catalytic performance at 60 °C and thermal stability up to 40 °C. Hydrolysis of highly deacetylated chitosan (98% DDA) primarily yielded $(GlcN)_2$ and $(GlcN)_3$ oligomers, which confirms the enzyme's suitability for targeted COS production from low-cost marine substrates [35]. In a comparable study, Nguyen et al. [99] optimized the culture conditions for chitosanase production by *Bacillus subtilis* using soybean meal hydrolysate (SMH) as a nitrogen source. While microbial enhancement of chitosanase activity is well documented, there is a scarcity of reports focusing on the utilization of inexpensive substrates such as SMH. Incorporation of SMH led to an 11.5-fold increase in enzyme activity, with recombinant *B. subtilis* PT5(MT1-Csn) achieving 1018.58 U/mL compared to 88.63 U/mL in the wild-type strain. The recombinant enzyme exhibited stability over a wide pH range (3.0–9.0) and retained maximal activity below 50 °C. Hydrolysis products predominantly included $(GlcN)_2$, $(GlcN)_3$, and $(GlcN)_4$, indicating efficient COS generation. This strategy not only reduces production costs significantly but also enhances the valorization of SMH as a substrate, highlighting the promise of *B. subtilis* PT5(MT1-Csn) as a cost-effective chitosanase producer for industrial COS synthesis. Overall, these studies demonstrate the potential of diverse low-cost substrates, ranging from agro-industrial residues to seafood by-products, in supporting economically viable microbial chitosanase production. Furthermore, the bioactive COSs generated via these fermentation systems offer promising applications in pharmaceutical, nutraceutical, and food industries. This potential is consistent with the goals of sustainable and circular bioeconomy development.

6.2. Immobilized Systems and Nano-Bbiocatalysts

Immobilization technologies and nano-biocatalyst systems for chitosanolytic enzymes offer promising avenues to improve the operational stability, reusability, and performance of chitosanases in continuous or repeated-use bioprocesses for COS production. These approaches facilitate enzyme recovery, reduce degradation, and enable applications under harsh process conditions. Moreover, nanoscale materials provide unique microenvironments that can modulate enzyme activity and substrate accessibility. Current advancements

in immobilized chitosanase systems and nanomaterial-assisted biocatalysts are reviewed with a focus on their roles in green and efficient enzymatic conversions.

In a recent study by De Medeiros Dantas et al. [100], chitosanase derived from *Bacillus toyonensis*, together with commercial cellulase and β-glucosidase, was comparatively immobilized using two distinct approaches: physical adsorption and covalent bonding onto solid supports. Among these enzymes, chitosanase exhibited optimal adsorption at 25 U/gsupport and demonstrated the best performance under covalent immobilization at 50 U/gsupport with 0.5% (*v*/*v*) glutaraldehyde, indicating its compatibility with both immobilization strategies. Overall, covalent bonding conferred greater stability than adsorption for all three enzymes. Notably, chitosanase immobilized via adsorption retained 70% of its initial activity after six hydrolysis cycles, outperforming previously reported systems such as that of El-Sayed et al. [101], where only 20% of enzymatic activity was preserved after six 1 h cycles using covalent immobilization. Complementing these findings, a novel immobilized chitosanase system was developed by covalently attaching chitosanase from *Bacillus pumilus* onto agar gel particles embedded with 200 nm magnetite nanoparticles. The magnetite–agar beads (average diameter: 338 μm) were prepared via emulsification and glyoxyl-mediated activation. These beads provided improved catalytic stability and reusability for chitosan hydrolysis. Although the specific activity of the immobilized enzyme was reduced to 16% relative to the free form, the immobilized chitosanase displayed markedly enhanced thermal stability, with a deactivation rate constant at 35 °C (3.9×10^{-8}/s) significantly lower than that of the free enzyme (8.1×10^{-5}/s). The immobilized system also enabled facile magnetic recovery and showed excellent reusability, which retains 80% of its initial activity after 10 hydrolysis cycles at 75 °C and pH 5.6. Moreover, the hydrolysis process yielded COSs with DP ranging from 2 to 7, with approximately 50% of the products comprising high-DP (≥5) COSs known for their physiological activity [102]. In another study, chitosanase from *Streptomyces albolongus* was immobilized onto Fe_3O_4–SiO_2 magnetic nanoparticles (MNPs) through covalent bonding. The MNPs were synthesized using a co-precipitation method, coated with silica via a sol–gel process, and amino-functionalized using 3-aminopropyltriethoxysilane. The resulting immobilized chitosanase system (MNPs@chitosanase) exhibited markedly enhanced stability compared to the free enzyme. Under thermal stress at 50 °C for 50 h, the immobilized enzyme maintained 19.4% residual activity, whereas the free enzyme retained only 8.4%. In addition, during chitosan hydrolysis, the immobilized chitosanase demonstrated improved catalytic efficiency, producing 79.4 μmol of COSs after 240 min, which is 1.4 times higher than the 56.8 μmol generated by the free enzyme under the same conditions. Furthermore, after 10 reuse cycles, the immobilized chitosanase retained 43.7% of its initial activity [103].

Overall, regardless of the immobilization strategy employed, including physical adsorption, covalent bonding, or incorporation into magnetic nanoparticle-based supports, chitosanases consistently demonstrate enhanced hydrolytic performance, stability, and reusability. These improvements could be adapted for other enzymes in biomass processes and highlight the strong potential of immobilized chitosanase systems for sustainable and scalable COS production in industrial applications.

6.3. Bioprocess of COS Production

Shrimp and crab are important aquatic food products and also serve as raw materials for some processed seafood items. However, their shell waste accounts for a significant proportion of their total weight, generating significant quantities of waste annually. In the past, much of this waste was simply discarded, causing environmental pollution, or processed into fishmeal and fish feed, resulting in limited economic benefits. Effectively utilizing this waste to create high-value products would not only address the waste problem but

also enhance its economic value. With proper separation and purification, approximately 20–35% chitin can be extracted from shrimp and crab shell waste, or from squid sheaths. The production of chitin generally involves deproteinization, which removes proteins from shells, and demineralization, which eliminates calcium carbonate and other minerals. Subsequent deacetylation of chitin, usually achieved by alkali treatment, yields chitosan. Using these materials to prepare chitin and chitosan can significantly increase the value of these wastes [104].

Chitosan has the potential to lower blood cholesterol, fight tumors, and enhance immunity, but its application in food applications still faces numerous challenges. First, chitosan has poor water solubility and dissolves only in acidic solutions, which can alter the pH, flavor, and texture of foods and make it unsuitable for neutral foods. Second, its solution viscosity is high, making it unsuitable for low-viscosity foods. Furthermore, chitosan can agglutinate proteins, potentially causing them to coagulate or precipitate, affecting food quality. Chitosan's high molecular weight makes it difficult to disperse in highly viscous or solid foods. In addition, chitosan has an astringent taste and can form a film in the mouth, affecting taste. These characteristics limit the widespread use of chitosan in food. However, chitosan hydrolysates have a lower molecular weight, resulting in reduced viscosity and increased water solubility. When hydrolyzed to a certain degree, chitosan does not coagulate or precipitate with food proteins and does not present astringency issues. Furthermore, even lower molecular weight oligosaccharides offer a refreshing sweetness, potentially making chitosan suitable for food processing.

COSs, composed of D-glucosamine linked via β-1,4 bonds, are obtained from chitosan via chemical or enzymatic hydrolysis. Their water solubility and low molecular weight offer advantages for commercial applications. COSs are important in food and agriculture, and they also have applications in healthcare. COSs have been reported to prevent tumor growth, treat asthma, improve bone strength, and prevent malaria, and can be used as gene delivery vectors in gene therapy [105]. The biological activities of COSs include antibacterial, antifungal, antiviral, antitumor, antioxidant, immunomodulatory, fat-depleting, blood pressure-control, and cholesterol-lowering properties [106]. COSs can be produced using either acid hydrolysis or enzymatic hydrolysis. Acid hydrolysis of chitosan using hydrochloric acid is the most widely used method. This method offers advantages of low cost and ease of operation. However, acid hydrolysis requires high temperatures and large amounts of acid, which can cause environmental pollution and energy consumption. Acid hydrolysis is a random hydrolysis process, making the degree of hydrolysis difficult to control, and the products are mostly GlcN. Enzymatic hydrolysis, on the other hand, utilizes chitosanase to hydrolyze chitosan. Due to the enzyme's specificity, the hydrolysis reaction is easy to control and relatively fast, saving time and reducing environmental pollution, making it a preferred method for hydrolyzing chitosan.

Microbial chitosanases can be used to produce COSs from chitosan at relatively high concentrations. Through endo- and exo-enzymatic activity, chitosanase hydrolyzes chitosan, particularly highly deacetylated chitosan, to form COSs with $(GlcN)_2$, $(GlcN)_3$, and $(GlcN)_4$ as the main products. However, large-scale application is limited because chitosanases are highly specific to chitosan and remain costly to produce. This makes strategies for enzyme recovery and reuse particularly important for industrial COS production. Immobilization of chitosanase can significantly improve its thermal and operational stability. For example, the immobilized chitosanase prepared by adsorption retained 70% of its activity after six hydrolysis cycles [100]. Partial hydrolysis of chitosan (PHC) in a batch reactor significantly reduced viscosity, facilitating substrate flow and enhancing productivity in the packed-bead reactor with immobilized chitosanase. This dual-reactor system represents a promising strategy for continuous COS production and can be applied to other viscous biopoly-

mers [107]. On the other hands, the ultrafiltration membrane reactor enabled simultaneous hydrolysis and product separation, preventing over-degradation of chitooligosaccharides and improved yield and selectivity. It also helped in retaining enzyme's activity for repeated use, reducing production costs, while allowing continuous operation with controlled molecular weight distribution. Kuo et al. [108] used crude chitosanase from *Bacillus cereus* NTU-FC-4 to hydrolyze chitosan to produce COSs in a membrane reactor. The main COSs produced in the reactor were $(GlcN)_2$, $(GlcN)_3$, $(GlcN)_4$, (GlcN)5, and (GlcN)6. The main drawback of ultrafiltration membrane reactors for COS production is membrane fouling, which leads to reduced permeability and decreased productivity [109]. Jeon and Kim used a dual reactor system combining an enzyme-packed column and a UF membrane reactor that enabled continuous COS production from chitosan, with 5 mL/min PHC providing optimal efficiency and minimal fouling [110]. Bioprocesses for COS production are now available, but they remain challenging to fully exploit. Scaling up purification methods to an economically acceptable level is another major obstacle.

7. Conclusions and Future Perspectives

Chitosanases are essential biocatalysts for converting chitosan into value-added COSs, whose structure-dependent bioactivities support broad applications in agriculture, food, biomedicine, and environmental biotechnology. Over the past decade, significant advancements have been made in understanding the catalytic mechanisms and structure-function relationships of chitosanases across various GH families, particularly GH8, GH46, GH5, and GH75. The identification of active-site architectures and subsite configurations has clarified the molecular basis for substrate selectivity and product specificity, laying the groundwork for targeted enzyme engineering. Consequently, an increasing number of chitosanases with desirable catalytic features have been discovered, enabling their significant contribution to biotechnological processes, particularly in the production of functional COSs. High-purity COSs can be achieved through appropriate separation and purification techniques. In addition, as key biological functions of COSs are being unveiled, their applications are expanding rapidly.

Despite these advancements, several challenges remain. The detailed molecular mechanisms underlying the endo-/exo-activity switching, substrate transglycosylation, and product pattern control are still not fully understood, particularly in underexplored GH families. In addition, discrepancies often exist between in vitro biochemical characterization and in vivo functional relevance, highlighting the need for integrative approaches that couple structural biology with systems-level analysis. Another unresolved issue lies in scaling laboratory findings to industrially robust processes, where enzyme stability, reusability, and cost-effectiveness must be rigorously addressed under complex feedstocks and processing environments. Furthermore, the diversity of COS structures has not yet been systematically linked to their bioactivities, leaving gaps in the rational design of COS-based products with predictable functionality.

Future directions should therefore prioritize the discovery of novel chitosanases from extremophilic or uncultured microorganisms using metagenomic, combined with machine learning-guided mining to predict functional diversity. Systems and synthetic biology strategies offer opportunities to engineer optimized expression hosts and metabolic pathways for sustainable production. Integrating continuous bioprocessing with advanced separation technologies may enhance scalability, while elucidating COS structure–activity relationships will be essential for their rational deployment in food, biomedical, and packaging applications. Achieving these goals will require interdisciplinary collaboration across enzyme science, computational modeling, materials chemistry, and process engineering.

Author Contributions: Conceptualization, O.T.K.N. and C.-H.K.; Validation, P.N.; Writing–Original Draft Preparation, O.T.K.N.; Writing–Review & Editing, Y.-C.L. and C.-H.K.; Resources, C.-J.S.; Visualization, O.T.K.N. and P.-T.C.; Supervision, C.-H.K.; Funding Acquisition, C.-H.K. All authors have read and agreed to the published version of the manuscript.

Funding: This work was supported by research funding grants provided by the National Science and Technology Council of Taiwan (MOST 111-2221-E-992-005-MY3).

Data Availability Statement: No new data were created or analyzed in this study. Data sharing is not applicable to this article.

Acknowledgments: The authors would like to acknowledge the Ministry of Education for providing the Taiwan Elite Scholarship.

Conflicts of Interest: The authors declare no conflicts of interest.

References

1. Doan, C.T.; Tran, T.N.; Nguyen, A.D.; Wang, S.-L. Enzymatic Production of Chitooligosaccharide Using a GH Family 46 Chitosanase from *Paenibacillus elgii* and Its Antioxidant Activity. *Catalysts* **2024**, *14*, 761. [CrossRef]
2. Li, B.; Cui, J.; Xu, T.; Xu, Y.; Long, M.; Li, J.; Liu, M.; Yang, T.; Du, Y.; Xu, Q. Advances in the preparation, characterization, and biological functions of chitosan oligosaccharide derivatives: A review. *Carbohydr. Polym.* **2024**, *332*, 121914. [CrossRef]
3. Weikert, T.; Niehues, A.; Cord-Landwehr, S.; Hellmann, M.J.; Moerschbacher, B.M. Reassessment of chitosanase substrate specificities and classification. *Nat. Commun.* **2017**, *8*, 1–11. [CrossRef]
4. Seki, K.; Nishiyama, Y.; Mitsutomi, M. Characterization of a novel exo-chitosanase, an exo-chitobiohydrolase, from Gongronella butleri. *J. Biosci. Bioeng.* **2019**, *127*, 425–429. [CrossRef]
5. Tong, L.; Li, Y.; Qin, Q.; Yu, Y.; Duan, L.; Wang, X.; Jiang, Y.; Liao, G.; Zhang, Y.; Wu, C.; et al. Enhancing activity and stability of a GH8 chitosanase through conserved N-terminal and peripheral residue mutations for bioactive chitooligosaccharide production. *Int. J. Biol. Macromol.* **2025**, *315*, 144643. [CrossRef]
6. Zhou, Z.; Wang, X. Improve thermostability of *Bacillus* sp. TS chitosanase through structure-based alignment. *Sci. Rep.* **2021**, *11*, 1–9. [CrossRef]
7. Bhuvanachandra, B.; Sivaramakrishna, D.; Alim, S.; Preethiba, G.; Rambabu, S.; Swamy, M.J.; Podile, A.R. New Class of Chitosanase from *Bacillus amyloliquefaciens* for the Generation of Chitooligosaccharides. *J. Agric. Food Chem.* **2021**, *69*, 78–87. [CrossRef] [PubMed]
8. Guo, J.; Wang, Y.; Zhang, X.; Gao, W.; Cai, Z.; Hong, T.; Man, Z.; Qing, Q. Improvement of the Catalytic Activity of Chitosanase BsCsn46A from *Bacillus subtilis* by Site-Saturation Mutagenesis of Proline121. *J. Agric. Food Chem.* **2021**, *69*, 11835–11846. [CrossRef] [PubMed]
9. Wu, C.; Yu, X.; Zheng, P.; Chen, P.; Wu, D. Rational Redesign of Chitosanase to Enhance Thermostability and Catalytic Activity to Produce Chitooligosaccharides with a Relatively High Degree of Polymerization. *J. Agric. Food Chem.* **2023**, *71*, 15213–15223. [CrossRef]
10. Sun, H.; Cheng, Y.; Zhao, L.; Cao, R. Improvement of the catalytic performance of chitosanase Csn-PD from Paenibacillus dendritiformis by semi-rational design. *Int. J. Biol. Macromol.* **2024**, *264*, 130753. [CrossRef] [PubMed]
11. Gao, W.; Ding, F.; Wu, J.; Ma, W.; Wang, C.; Man, Z.; Cai, Z.; Guo, J. Modulation of a Loop Region in the Substrate Binding Pocket Affects the Degree of Polymerization of *Bacillus subtilis* Chitosanase Products. *J. Agric. Food Chem.* **2024**, *72*, 4358–4366. [CrossRef]
12. Duan, S.Y.; Zhang, X.S.; Yuan, Y.Q.; Jing, S.Y.; Qiao, M.H.; Ji, R. Improving the Thermostability and Catalytic Performance of the Bacillus subtilis Chitosanase BsCsn46A via Computational Design. *Appl. Biochem. Microbiol.* **2024**, *60*, 889–896. [CrossRef]
13. Wang, Q.; Liu, S.; Li, K.; Xing, R.; Chen, X.; Li, P. A Computational Biology Study on the Structure and Dynamics Determinants of Thermal Stability of the Chitosanase from *Aspergillus fumigatus*. *Int. J. Mol. Sci.* **2023**, *24*, 6671. [CrossRef]
14. Xie, J.; Liu, J.; Wang, S.; Wang, G. Improved Enzymatic Properties of Chitosanase CsnMY002 from *Bacillus subtilis* via Computational Design. *Int. J. Mol. Sci.* **2025**, *26*, 1588. [CrossRef]
15. Yang, H.; Wang, L.; Xu, C.; Hao, W.; Xing, R.; Liu, S.; Yu, H.; Li, P. Screening for Aspergillus fumigatus strain-2T-2 with high chitosanase production activity and its application in chitosan degradation. *Electron. J. Biotechnol.* **2024**, *68*, 57–66. [CrossRef]
16. Jung, W.-J.; Kuk, J.-H.; Kim, K.-Y.; Jung, K.-C.; Park, R.-D. Purification and characterization of exo-β-d-glucosaminidase from Aspergillus fumigatus S-26. *Protein Expr. Purif.* **2006**, *45*, 125–131. [CrossRef]
17. Akram, F.; Haq, I.U.; Aqeel, A.; Ahmed, Z.; Shah, F.I. Thermostable cellulases: Structure, catalytic mechanisms, directed evolution and industrial implementations. *Renew. Sustain. Energy Rev.* **2021**, *151*. [CrossRef]
18. Xu, Y.; Li, L.; Cao, S.; Zhu, B.; Yao, Z. An updated comprehensive review of advances on structural features, catalytic mechanisms, modification methods and applications of chitosanases. *Process. Biochem.* **2022**, *118*, 263–273. [CrossRef]

19. Santos-Moriano, P.; Kidibule, P.E.; Alleyne, E.; Ballesteros, A.O.; Heras, A.; Fernandez-Lobato, M.; Plou, F.J. Efficient conversion of chitosan into chitooligosaccharides by a chitosanolytic activity from Bacillus thuringiensis. *Process. Biochem.* **2018**, *73*, 102–108. [CrossRef]
20. Izume, M.; Nagae, S.I.; Kawagishi, H.; Mitsutomi, M.; Ohtakara, A. Action pattern of Bacillus sp. No. 7-M chitosanase on partially N-acetylated chitosan. *Biosci. Biotechnol. Biochem.* **1992**, *56*, 448–453. [CrossRef]
21. Singh, R.; Weikert, T.; Basa, S.; Moerschbacher, B.M. Structural and biochemical insight into mode of action and subsite specificity of a chitosan degrading enzyme from Bacillus spec. MN. *Sci. Rep.* **2019**, *9*, 1–13. [CrossRef]
22. Wang, Y.; Qin, Z.; Fan, L.; Zhao, L. Structure–function analysis of Gynuella sunshinyii chitosanase uncovers the mechanism of substrate binding in GH family 46 members. *Int. J. Biol. Macromol.* **2020**, *165*, 2038–2048. [CrossRef]
23. Su, H.; Zhao, H.; Jia, Z.; Guo, C.; Sun, J.; Mao, X. Biochemical Characterization of a GH46 Chitosanase Provides Insights into the Novel Digestion Specificity. *J. Agric. Food Chem.* **2023**, *71*, 2038–2048. [CrossRef] [PubMed]
24. Su, H.; Sun, J.; Chu, W.; Yuan, B.; Mao, X. Biochemical characterization and cleavage pattern analysis of a novel chitosanase with cellulase activity. *Appl. Microbiol. Biotechnol.* **2022**, *106*, 1979–1990. [CrossRef] [PubMed]
25. Jiang, Z.; Ma, S.; Guan, L.; Yan, Q.; Yang, S. Biochemical characterization of a novel bifunctional chitosanase from Paenibacillus barengoltzii for chitooligosaccharide production. *World J. Microbiol. Biotechnol.* **2021**, *37*, 1–13. [CrossRef]
26. Wang, S.-L.; Peng, J.-H.; Liang, T.-W.; Liu, K.-C. Purification and characterization of a chitosanase from *Serratia marcescens* TKU011. *Carbohydr. Res.* **2008**, *343*, 1316–1323. [CrossRef]
27. Wang, S.-L.; Tseng, W.-N.; Liang, T.-W. Biodegradation of shellfish wastes and production of chitosanases by a squid pen-assimilating bacterium, *Acinetobacter calcoaceticus* TKU024. *Biodegradation* **2011**, *22*, 939–948. [CrossRef] [PubMed]
28. Doan, C.T.; Tran, T.N.; Nguyen, V.B.; Tran, T.D.; Nguyen, A.D.; Wang, S.-L. Bioprocessing of Squid Pens Waste into Chitosanase by *Paenibacillus* sp. TKU047 and Its Application in Low-Molecular Weight Chitosan Oligosaccharides Production. *Polymers* **2020**, *12*, 1163. [CrossRef]
29. Doan, C.T.; Tran, T.N.; Wen, I.-H.; Nguyen, V.B.; Nguyen, A.D.; Wang, S.-L. Conversion of Shrimp Head Waste for Production of a Thermotolerant, Detergent-Stable, Alkaline Protease by *Paenibacillus* sp. *Catalysts* **2019**, *9*, 798. [CrossRef]
30. Wang, Y.; Mo, H.; Hu, Z.; Liu, B.; Zhang, Z.; Fang, Y.; Hou, X.; Liu, S.; Yang, G. Production, Characterization and Application of a Novel Chitosanase from Marine Bacterium *Bacillus paramycoides* BP-N07. *Foods* **2023**, *12*, 3350. [CrossRef]
31. Zheng, Q.; Meng, X.; Cheng, M.; Li, Y.; Liu, Y.; Chen, X. Cloning and Characterization of a New Chitosanase From a Deep-Sea *Bacterium Serratia* sp. QD07. *Front. Microbiol.* **2021**, *12*. [CrossRef]
32. Zhang, R.-X.; Wu, Z.-W.; Zhang, S.-J.; Wei, H.-M.; Hua, C.-W.; Li, L.; Yang, T.-Y. Gene cloning and molecular characterization of a thermostable chitosanase from *Bacillus cereus* TY24. *BMC Biotechnol.* **2022**, *22*, 1–12. [CrossRef]
33. Chulhong, O.; Zoysa, M.D.; Kang, D.-H.; Lee, Y.-D.; Whang, I.-S.; Nikapitiya, C.; Heo, S.-J.; Yoon, K.-T.; Affan, A.; Lee, J.-H. Isolation, purification, and enzymatic characterization of extracellular chitosanase from marine bacterium *Bacillus subtilis* CH2. *Appl. Biochem. Biotechnol.* **2011**, *21*, 1021–1025.
34. Doan, C.T.; Tran, T.N.; Nguyen, V.B.; Nguyen, A.D.; Wang, S.-L. Production of a Thermostable Chitosanase from Shrimp Heads via *Paenibacillus mucilaginosus* TKU032 Conversion and its Application in the Preparation of Bioactive Chitosan Oligosaccharides. *Mar. Drugs* **2019**, *17*, 217. [CrossRef]
35. Doan, C.T.; Tran, T.N.; Tran, T.P.H.; Nguyen, T.T.; Nguyen, H.K.; Tran, T.K.T.; Vu, B.T.; Trinh, T.H.T.; Nguyen, A.D.; Wang, S.-L. Chitosanase Production from the Liquid Fermentation of Squid Pens Waste by *Paenibacillus elgii*. *Polymers* **2023**, *15*, 3724. [CrossRef]
36. Zhang, C.; Li, Y.; Zhang, T.; Zhao, H. Increasing chitosanase production in *Bacillus cereus* by a novel mutagenesis and screen method. *Bioengineered* **2021**, *12*, 266–277. [CrossRef] [PubMed]
37. Cao, S.; Gao, P.; Xia, W.; Liu, S.; Wang, B. A Novel Chitosanase from *Penicillium oxalicum* M2 for Chitooligosaccharide Production: Purification, Identification and Characterization. *Mol. Biotechnol.* **2022**, *64*, 947–957. [CrossRef] [PubMed]
38. Nguyen, A.D.; Huang, C.-C.; Liang, T.-W.; Nguyen, V.B.; Pan, P.-S.; Wang, S.-L. Production and purification of a fungal chitosanase and chitooligomers from *Penicillium janthinellum* D4 and discovery of the enzyme activators. *Carbohydr. Polym.* **2014**, *108*, 331–337. [CrossRef] [PubMed]
39. Abedin, R.M.A.; Elwaly, D.R.M.A.; El-Salam, A.E.A. Production, statistical evaluation and characterization of chitosanase from *Fusarium oxysporum* D18. *Ann. Microbiol.* **2023**, *73*, 1–14. [CrossRef]
40. Shehata, A.N.; Abeer, A.A.E.A. Improved production and partial characterization of chitosanase from a newly isolated *Chaetomium globosum* KM651986 and its application for chitosan oligosaccharides. *J. Chem. Pharm. Res.* **2015**, *7*, 727–740.
41. Sinha, S.; Tripathi, P.; Chand, S. A New Bifunctional Chitosanase Enzyme from *Streptomyces* sp. and Its Application in Production of Antioxidant Chitooligosaccharides. *Appl. Biochem. Biotechnol.* **2012**, *167*, 1029–1039. [CrossRef]
42. Jiang, X.; Chen, D.; Chen, L.; Yang, G.; Zou, S. Purification, characterization, and action mode of a chitosanase from *Streptomyces roseolus* induced by chitin. *Carbohydr. Res.* **2012**, *355*, 40–44. [CrossRef]

43. Vanathia, P.; Premasudha, P.; Rajendran, D.R. Production and Characterization of Chitosanase Enzyme from *Streptomyces* sp. Isolated from Biowaste Soil Samples. *IJPBS.* **2016**, *7*, 302–313.
44. Cai, D.; Rao, Y.; Zhan, Y.; Wang, Q.; Chen, S. Engineering *Bacillus* for efficient production of heterologous protein: Current progress, challenge and prospect. *J. Appl. Microbiol.* **2019**, *126*, 1632–1642. [CrossRef] [PubMed]
45. Rosano, G.L.; Ceccarelli, E.A. Recombinant protein expression in *Escherichia coli*: Advances and challenges. *Front. Microbiol.* **2014**, *5*, 172. [CrossRef]
46. Zhang, K.; Su, L.; Wu, J. Recent Advances in Recombinant Protein Production by *Bacillus subtilis*. *Annu. Rev. Food Sci. Technol.* **2020**, *11*, 295–318. [CrossRef]
47. Yang, Z.; Zhang, Z. Engineering strategies for enhanced production of protein and bio-products in *Pichia pastoris*: A review. *Biotechnol. Adv.* **2018**, *36*, 182–195. [CrossRef]
48. Su, H.; Sun, J.; Guo, C.; Jia, Z.; Mao, X. Heterogenously-expressed chitosanase combining a green ball milling method for enzymatic degradation. *Food Bioeng.* **2022**, *1*, 37–46. [CrossRef]
49. Qin, Z.; Chen, Q.; Lin, S.; Luo, S.; Qiu, Y.; Zhao, L. Expression and characterization of a novel cold-adapted chitosanase suitable for chitooligosaccharides controllable preparation. *Food Chem.* **2018**, *253*, 139–147. [CrossRef] [PubMed]
50. Guo, N.; Sun, J.; Wang, W.; Gao, L.; Liu, J.; Liu, Z.; Xue, C.; Mao, X. Cloning, expression and characterization of a novel chitosanase from *Streptomyces albolongus* ATCC 27414. *Food Chem.* **2019**, *286*, 696–702. [CrossRef]
51. Xu, Y.; Wang, H.; Zhu, B.; Yao, Z.; Jiang, L. Purification and biochemical characterization of a novel chitosanase cloned from the gene of *Kitasatospora setae* KM-6054 and its application in the production of chitooligosaccharides. *World J. Microbiol. Biotechnol.* **2023**, *39*, 1–10. [CrossRef]
52. Gu, Y.; Xu, X.; Wu, Y.; Niu, T.; Liu, Y.; Li, J.; Du, G.; Liu, L. Advances and prospects of *Bacillus subtilis* cellular factories: From rational design to industrial applications. *Metab. Eng.* **2018**, *50*, 109–121. [CrossRef]
53. Su, P.-C.; Hsueh, W.-C.; Chang, W.-S.; Chen, P.T. Enhancement of chitosanase secretion by *Bacillus subtilis* for production of chitosan oligosaccharides. *J. Taiwan Inst. Chem. Eng.* **2017**, *79*, 49–54. [CrossRef]
54. Kang, L.-X.; Chen, X.-M.; Fu, L.; Ma, L.-X. Recombinant expression of chitosanase from *Bacillus subtilis* HD145 in Pichia pastoris. *Carbohydr. Res.* **2012**, *352*, 37–43. [CrossRef]
55. Zhou, J.; Liu, X.; Yuan, F.; Deng, B.; Yu, X. Biocatalysis of Heterogenously-Expressed Chitosanase for the Preparation of Desirable Chitosan Oligosaccharides Applied against Phytopathogenic Fungi. *ACS Sustain. Chem. Eng.* **2020**, *8*, 4781–4791. [CrossRef]
56. Luo, S.; Qin, Z.; Chen, Q.; Fan, L.; Jiang, L.; Zhao, L. High level production of a *Bacillus amlyoliquefaciens* chitosanase in *Pichia pastoris* suitable for chitooligosaccharides preparation. *Int. J. Biol. Macromol.* **2020**, *149*, 1034–1041. [CrossRef] [PubMed]
57. Zhang, W.; Zhou, J.; Gu, Q.; Sun, R.; Yang, W.; Lu, Y.; Wang, C.; Yu, X. Heterologous expression of GH5 chitosanase in *Pichia pastoris* and antioxidant biological activity of its chitooligosacchride hydrolysate. *J. Biotechnol.* **2022**, *348*, 55–63. [CrossRef]
58. Ding, M.; Zhang, T.; Sun, C.; Zhang, H.; Zhang, Y. A Chitosanase mutant from *Streptomyces* sp. N174 prefers to produce functional chitopentasaccharide. *Int. J. Biol. Macromol.* **2020**, *151*, 1091–1098. [CrossRef]
59. Sun, H.; Cao, R.; Li, L.; Zhao, L.; Liu, Q. Cloning, purification and characterization of a novel GH46 family chitosanase, Csn-CAP, from Staphylococcus capitis. *Process. Biochem.* **2018**, *75*, 146–151. [CrossRef]
60. Yang, G.; Sun, H.; Cao, R.; Liu, Q.; Mao, X. Characterization of a novel glycoside hydrolase family 46 chitosanase, Csn-BAC, from *Bacillus* sp. MD-5. *Int. J. Biol. Macromol.* **2020**, *146*, 518–523. [CrossRef] [PubMed]
61. Sun, H.; Mao, X.; Guo, N.; Zhao, L.; Cao, R.; Liu, Q. Discovery and Characterization of a Novel Chitosanase from *Paenibacillus dendritiformis* by Phylogeny-Based Enzymatic Product Specificity Prediction. *J. Agric. Food Chem.* **2018**, *66*, 4645–4651. [CrossRef]
62. Saito, A.; Ooya, T.; Miyatsuchi, D.; Fuchigami, H.; Terakado, K.; Nakayama, S.-y.; Watanabe, T.; Nagata, Y.; Ando, A. Molecular characterization and antifungal activity of a family 46 chitosanase from *Amycolatopsis* sp. CsO-2. *FEMS Microbiol. Lett.* **2009**, *293*, 79–84. [CrossRef]
63. Qin, Z.; Luo, S.; Li, Y.; Chen, Q.; Qiu, Y.; Zhao, L.; Jiang, L.; Zhou, J. Biochemical properties of a novel chitosanase from *Bacillus amyloliquefaciens* and its use in membrane reactor. *LWT.* **2018**, *97*, 9–16. [CrossRef]
64. Wang, Y.; Zhao, Y.; Li, J.; Zong, H.; Chen, Y.; Zhou, J.; Li, X.; Ye, X. Characterization of a Novel Acid-Stable Chitosanase from *Lentinula edodes* Suitable for Chitooligosaccharide Preparation. *Foods* **2024**, *13*, 3127. [CrossRef] [PubMed]
65. Liu, Y.; Li, Y.; Tong, S.; Yuan, M.; Wang, X.; Wang, J.; Fan, Y. Expression of a Beauveria bassiana chitosanase (BbCSN-1) in Pichia pastoris and enzymatic analysis of the recombinant protein. *Protein Expr. Purif.* **2020**, *166*, 105519. [CrossRef] [PubMed]
66. Zhang, J.; Cao, H.; Li, S.; Zhao, Y.; Wang, W.; Xu, Q.; Du, Y.; Yin, H. Characterization of a new family 75 chitosanase from *Aspergillus* sp. W-2. *Int. J. Biol. Macromol.* **2015**, *81*, 362–369. [CrossRef]
67. Yang, Y.; Zheng, Z.; Xiao, Y.; Zhang, J.; Zhou, Y.; Li, X.; Li, S.; Yu, H. Cloning and Characterization of a Cold-adapted Chitosanase from Marine Bacterium *Bacillus* sp. BY01. *Molecules* **2019**, *24*, 3915. [CrossRef]
68. Cao, S.; Gao, P.; Xia, W.; Liu, S.; Liu, X. Cloning and characterization of a novel GH75 family chitosanase from *Penicillium oxalicum* M2. *Process. Biochem.* **2022**, *120*, 41–52. [CrossRef]

69. Su, H.; Sun, J.; Guo, C.; Wang, Y.; Secundo, F.; Dong, H.; Mao, X. Structure-based mining of a chitosanase with distinctive degradation mode and product specificity. *Appl. Microbiol. Biotechnol.* **2023**, *107*, 6859–6871. [CrossRef]
70. Li, Y.; Gou, Y.; Liu, Z.; Xie, T.; Wang, G. Structure-based rational design of chitosanase CsnMY002 for high yields of chitobiose. *Colloid Surface B.* **2021**, *202*, 111692. [CrossRef]
71. Cui, D.; Yang, J.; Lu, B.; Shen, H. Efficient Preparation of Chitooligosaccharide With a Potential Chitosanase Csn-SH and Its Application for Fungi Disease Protection. *Front. Microbiol.* **2021**, *12*, 682829. [CrossRef] [PubMed]
72. Wang, Y.; Li, D.; Liu, M.; Xia, C.; Fan, Q.; Li, X.; Lan, Z.; Shi, G.; Dong, W.; Li, Z.; et al. Preparation of Active Chitooligosaccharides with a Novel Chitosanase *Aq*CoA and Their Application in Fungal Disease Protection. *J. Agric. Food Chem.* **2021**, *69*, 3351–3361. [CrossRef] [PubMed]
73. Wang, J.; Wang, P.; Zhu, M.; Chen, W.; Yu, S.; Zhong, B. Overexpression and Biochemical Properties of a GH46 Chitosanase From Marine *Streptomyces hygroscopicus* R1 Suitable for Chitosan Oligosaccharides Preparation. *Front. Microbiol.* **2022**, *12*, 816845. [CrossRef]
74. Lacombe-Harvey, M.; Fortin, M.; Ohnuma, T.; Fukamizo, T.; Letzel, T.; Brzezinski, R. A highly conserved arginine residue of the chitosanase from *Streptomyces* sp. N174 is involved both in catalysis and substrate binding. *BMC Biochem.* **2013**, *14*, 23. [CrossRef]
75. Takasuka, T.E.; Bianchetti, C.M.; Tobimatsu, Y.; Bergeman, L.F.; Ralph, J.; Fox, B.G. Structure-guided analysis of catalytic specificity of the abundantly secreted chitosanase SACTE_5457 from *Streptomyces* sp. SirexAA-E. *Proteins: Struct. Funct. Genet.* **2014**, *82*, 1245–1257. [CrossRef] [PubMed]
76. Chen, T.; Cheng, G.; Jiao, S.; Ren, L.; Zhao, C.; Wei, J.; Han, J.; Pei, M.; Du, Y.; Li, J.-J. Expression and Biochemical Characterization of a Novel Marine Chitosanase from *Streptomyces niveus* Suitable for Preparation of Chitobiose. *Mar. Drugs* **2021**, *19*, 300. [CrossRef]
77. Guo, J.; Wang, Y.; Gao, W.; Wang, X.; Gao, X.; Man, Z.; Cai, Z.; Qing, Q. Gene Cloning, Functional Expression, and Characterization of a Novel GH46 Chitosanase from *Streptomyces avermitilis* (SaCsn46A). *Appl. Biochem. Biotechnol.* **2021**, *194*, 813–826. [CrossRef]
78. Zhou, Z.; Zhao, S.; Wang, S.; Li, X.; Su, L.; Ma, Y.; Li, J.; Song, J. Extracellular Overexpression of Chitosanase from *Bacillus* sp. TS in *Escherichia coli*. *Appl. Biochem. Biotechnol.* **2015**, *175*, 3271–3286. [CrossRef]
79. Chen, H.; Lin, B.; Zhang, R.; Gong, Z.; Wen, M.; Su, W.; Zhou, J.; Zhao, L.; Wang, J. Controllable preparation of chitosan oligosaccharides via a recombinant chitosanase from marine *Streptomyces lydicus* S1 and its potential application on preservation of pre-packaged tofu. *Front. Microbiol.* **2022**, *13*, 1007201. [CrossRef]
80. Aktuganov, G.E.; Safina, V.R.; Galimzianova, N.F.; Gilvanova, E.A.; Kuzmina, L.Y.; Melentiev, A.I.; Baymiev, A.H.; Lopatin, S.A. Constitutive chitosanase from *Bacillus thuringiensis* B-387 and its potential for preparation of antimicrobial chitooligomers. *World J. Microbiol. Biotechnol.* **2022**, *38*, 1–15. [CrossRef]
81. Wang, J.; Li, X.; Chen, H.; Lin, B.; Zhao, L. Heterologous Expression and Characterization of a High-Efficiency Chitosanase From *Bacillus mojavensis* SY1 Suitable for Production of Chitosan Oligosaccharides. *Front. Microbiol.* **2021**, *12*, 781138. [CrossRef] [PubMed]
82. Liaqat, F.; Akgün, I.H.; Khazi, M.I.; Eltem, R. Characterization of different chitosanases of *Bacillus* strains and their application in chitooligosaccharides production. *J. Basic Microbiol.* **2022**, *63*, 404–416. [CrossRef] [PubMed]
83. Lin, S.; Qin, Z.; Chen, Q.; Fan, L.; Zhou, J.; Zhao, L. Efficient Immobilization of Bacterial GH Family 46 Chitosanase by Carbohydrate-Binding Module Fusion for the Controllable Preparation of Chitooligosaccharides. *J. Agric. Food Chem.* **2019**, *67*, 6847–6855. [CrossRef]
84. Han, Y.; Gao, P.; Yu, W.; Lu, X. N-Terminal seven-amino-acid extension simultaneously improves the pH stability, optimal temperature, thermostability and catalytic efficiency of chitosanase CsnA. *Biotechnol. Lett.* **2017**, *40*, 75–82. [CrossRef]
85. Jia, Z.; Su, H.; Zhao, Q.; Wang, S.; Sun, J.; Mao, X. Structure-Assisted Design of Chitosanase Product Specificity for the Production of High-Degree Polymerization Chitooligosaccharides. *J. Agric. Food Chem.* **2024**, *72*, 19081–19092. [CrossRef]
86. Jing, G.; Wenjun, G.; Yi, W.; Kepan, X.; Wen, L.; Tingting, H.; Zhiqiang, C. Enhancing Enzyme Activity and Thermostability of Bacillus amyloliquefaciens Chitosanase BaCsn46A Through Saturation Mutagenesis at Ser196. *Curr. Microbiol.* **2023**, *80*, 1–10. [CrossRef] [PubMed]
87. Lu, J.; Wang, C.; Ma, Y.; Liu, K.; Fu, X.; Xing, S. Exploration of the Product Specificity of chitosanase CsnMY002 and Mutants Using Molecular Dynamics Simulations. *Molecules* **2023**, *28*, 1048. [CrossRef]
88. Guo, J.; Gao, W.; Zhang, X.; Pan, W.; Zhang, X.; Man, Z.; Cai, Z. Enhancing the thermostability and catalytic activity of *Bacillus subtilis* chitosanase by saturation mutagenesis of Lys242. *Biotechnol. J.* **2023**, *19*, e2300010. [CrossRef]
89. Zhou, J.; Gu, Q.; Shen, Y.; Harindintwali, J.D.; Yang, W.; Zou, S.; Han, M.; Ma, C.; Yu, X.; Liu, X. Enhancement of the performance of the GH75 family chitosanases by fusing a carbohydrate binding module and insights into their substrate binding mechanisms. *LWT.* **2022**, *163*, 113390. [CrossRef]
90. Guo, J.; Gao, W.; Wang, J.; Yao, Y.; Man, Z.; Cai, Z.; Qing, Q. Thr22 plays an important role in the efficient catalytic process of Bacillus subtilis chitosanase BsCsn46A. *Enzym. Microb. Technol.* **2023**, *167*, 110242. [CrossRef]

91. Han, Y.; Yu, R.; Gao, P.; Lu, X.; Yu, W. The hydrogen-bond network around Glu160 contributes to the structural stability of chitosanase CsnA from *Renibacterium* sp. QD1. *Int. J. Biol. Macromol.* **2018**, *109*, 880–887. [CrossRef]
92. Xu, K.; Fu, H.; Chen, Q.; Sun, R.; Li, R.; Zhao, X.; Zhou, J.; Wang, X. Engineering thermostability of industrial enzymes for enhanced application performance. *Int. J. Biol. Macromol.* **2024**, *291*, 139067. [CrossRef]
93. Wang, S.-L.; Liang, T.-W. Microbial reclamation of squid pens and shrimp shells. *Res. Chem. Intermed.* **2016**, *43*, 3445–3462. [CrossRef]
94. Li, K.C.; Xing, R.G.; Liu, S.; Qin, Y.K.; Yu, H.H.; Li, P.C. Size and pH effects of chitooligomers on antibacterial activity against *Staphylococcus aureus*. *Int. J. Biol. Macromol.* **2014**, *64*, 302–305. [CrossRef]
95. Zhai, X.; Li, C.; Ren, D.; Wang, J.; Ma, C.; El-Aty, A.A. The impact of chitooligosaccharides and their derivatives on the in vitro and in vivo antitumor activity: A comprehensive review. *Carbohydr. Polym.* **2021**, *266*, 118132. [CrossRef] [PubMed]
96. Huang, X.; Chen, M.; Wu, H.; Jiao, Y.; Zhou, C. Macrophage Polarization Mediated by Chitooligosaccharide (COS) and Associated Osteogenic and Angiogenic Activities. *ACS Biomater. Sci. Eng.* **2020**, *6*, 1614–1629. [CrossRef] [PubMed]
97. Xing, R.; Liu, Y.; Li, K.; Yu, H.; Liu, S.; Yang, Y.; Chen, X.; Li, P. Monomer composition of chitooligosaccharides obtained by different degradation methods and their effects on immunomodulatory activities. *Carbohydr. Polym.* **2017**, *157*, 1288–1297. [CrossRef]
98. de Andrade, R.C.L.C.; de Araújo, N.K.; Torres-Rêgo, M.; Furtado, A.A.; Daniele-Silva, A.; Paiva, W.d.S.; Dantas, J.M.d.M.; da Silva, N.S.; da Silva-Júnior, A.A.; Ururahy, M.A.G.; et al. Production and Characterization of Chitooligosaccharides: Evaluation of Acute Toxicity, Healing, and Anti-Inflammatory Actions. *Int. J. Mol. Sci.* **2021**, *22*, 10631. [CrossRef]
99. Nguyen, O.T.K.; Chen, P.-T.; Nargotra, P.; Chen, S.-C.; Cheng, C.-Y.; Wang, H.-M.D.; Liu, Y.-C.; Kuo, C.-H. Sustainable bacterial chitosanase production using soybean meal hydrolysate: Insights into biochemical and hydrolysis characteristics. *Process. Biochem.* **2025**, *150*, 202–212. [CrossRef]
100. Maria de Medeiros Dantas, J.M.; Silva, N.S.d; Padilha, C.E.d.A.; Kelly de Araújo, N.; Santos, E.S.D. Enhancing chitosan hydrolysis aiming chitooligosaccharides production by using immobilized chitosanolytic enzymes. *Biocatal. Agric. Biotechnol.* **2020**, *28*, 101759. [CrossRef]
101. El-Sayed, S.T.; Omar, N.I.; El-Sayed, E.-S.M.; Shousha, W.G. Kinetic and stability improvement of immobilized pepper chitosanase on chitin by covalent bond. *Saudi J. Med. Pharm. Sci.* **2017**, *3*, 957–965.
102. Kuroiwa, T.; Nakagawa, Y.; Takayanagi, R.; Kanazawa, A. Chitosanase-immobilized magnetite-agar gel particles as a highly stable and reusable biocatalyst for enhanced production of physiologically active chitosan oligosaccharides. *Enzym. Microb. Technol.* **2024**, *178*, 110443. [CrossRef]
103. Wang, W.; Guo, N.; Huang, W.; Zhang, Z.; Mao, X. Immobilization of Chitosanases onto Magnetic Nanoparticles to Enhance Enzyme Performance. *Catalysts* **2018**, *8*, 401. [CrossRef]
104. El Knidri, H.; Belaabed, R.; Addaou, A.; Laajeb, A.; Lahsini, A. Extraction, chemical modification and characterization of chitin and chitosan. *Int. J. Biol. Macromol.* **2018**, *120*, 1181–1189. [CrossRef] [PubMed]
105. Wang, J.; Zhang, J.; Song, F.; Gui, T.; Xiang, J. Purification and Characterization of Chitinases from Ridgetail White Prawn *Exopalaemon carinicauda*. *Molecules* **2015**, *20*, 1955–1967. [CrossRef]
106. Liaqat, F.; Eltem, R. Chitooligosaccharides and their biological activities: A comprehensive review. *Carbohydr. Polym.* **2018**, *184*, 243–259. [CrossRef] [PubMed]
107. Santos-Moriano, P.; Woodley, J.M.; Plou, F.J. Continuous production of chitooligosaccharides by an immobilized enzyme in a dual-reactor system. *J. Mol. Catal. B: Enzym.* **2016**, *133*, 211–217. [CrossRef]
108. Kuo, C.; Chen, C.; Chiang, B.H. Process Characteristics of Hydrolysis of Chitosan in a Continuous Enzymatic Membrane Reactor. *J. Food Sci.* **2004**, *69*, 332–337. [CrossRef]
109. Jung, W.-J.; Park, R.-D. Bioproduction of Chitooligosaccharides: Present and Perspectives. *Mar. Drugs* **2014**, *12*, 5328–5356. [CrossRef]
110. Jeon, Y.-J.; Kim, S.-K. Continuous production of chitooligosaccharides using a dual reactor system. *Process. Biochem.* **2000**, *35*, 623–632. [CrossRef]

Disclaimer/Publisher's Note: The statements, opinions and data contained in all publications are solely those of the individual author(s) and contributor(s) and not of MDPI and/or the editor(s). MDPI and/or the editor(s) disclaim responsibility for any injury to people or property resulting from any ideas, methods, instructions or products referred to in the content.